

1 **Title:** Essential role of Notch/Hes1 signaling in postnatal pancreatic exocrine development

2

3 **Short title:** Notch in pancreas maturation

4

5 Katsutoshi Kuriyama<sup>1</sup>, Yuzo Kodama<sup>1,2</sup>, Masahiro Shiokawa<sup>1</sup>, Yoshihiro Nishikawa<sup>1</sup>, Saiko  
6 Marui<sup>1</sup>, Takeshi Kuwada<sup>1</sup>, Yuko Sogabe<sup>1</sup>, Nobuyuki Kakiuchi<sup>1</sup>, Teruko Tomono<sup>1</sup>, Tomoaki  
7 Matsumori<sup>1</sup>, Atsushi Mima<sup>1</sup>, Toshihiro Morita<sup>1</sup>, Tatsuki Ueda<sup>1</sup>, Motoyuki Tsuda<sup>1</sup>, Yuki Yamauchi<sup>1</sup>,  
8 Yojiro Sakuma<sup>1</sup>, Yuji Ota<sup>1</sup>, Takahisa Maruno<sup>1</sup>, Norimitsu Uza<sup>1</sup>, Ryoichiro Kageyama<sup>3</sup>, Tsutomu  
9 Chiba<sup>1,4</sup>, and Hiroshi Seno<sup>1</sup>

10

11 <sup>1</sup>Department of Gastroenterology and Hepatology, Kyoto University Graduate School of Medicine,  
12 54 Kawahara-cho, Shogoin, Sakyo-ku, Kyoto, 606-8507, Japan.

13 <sup>2</sup>Department of Gastroenterology, Kobe University Graduate School of Medicine, 7-5-1 Kusunoki-  
14 cho, Chuo-ku, Kobe, Hyogo, 650-0017, Japan.

15 <sup>3</sup>Institute for Frontier Life and Medical Sciences, Kyoto University, 53 Shogoin Kawahara-cho,  
16 Sakyo-ku, Kyoto, 606-8507, Japan

17 <sup>4</sup>Kansai Electric Power Hospital, 2-1-7 Fukushima, Fukushima-ku, Osaka, 553-0003, Japan.

18

19 Correspondence: Yuzo Kodama

20 Department of Gastroenterology, Kobe University Graduate School of Medicine, 7-5-1 Kusunoki-  
21 cho, Chuo-ku, Kobe, Hyogo 650-0017, Japan.

22 E-mail: kodama@med.kobe-u.ac.jp

23 Phone: +81-78-382-6305

24 Fax: +81- 78-382-6309

25 **Abstract**

26 *Background* Notch/Hes1 signaling has been shown to play a role in determining the fate of  
27 pancreatic progenitor cells. However, its function in postnatal pancreatic maturation is not fully  
28 elucidated.

29 *Methods* We generated conditional *Hes1* knockout and/or Notch intracellular domain (NICD)  
30 overexpression mice in *Ptf1a*- or *Pdx1*-positive pancreatic progenitor cells and analyzed pancreatic  
31 tissues.

32 *Results* Both *Ptf1a<sup>cre/+</sup>;Hes1<sup>ff</sup>* and *Ptf1a<sup>cre/+</sup>;Rosa26<sup>NICD</sup>* mice showed normal pancreatic  
33 development at P0. However, exocrine tissue of the pancreatic tail in *Ptf1a<sup>cre/+</sup>;Hes1<sup>ff</sup>* mice  
34 atrophied and was replaced by fat tissue by 4 weeks of age, with increased apoptotic cells and  
35 fewer centroacinar cells. This impaired exocrine development was completely rescued by NICD  
36 overexpression in *Ptf1a<sup>cre/+</sup>;Hes1<sup>ff</sup>;Rosa26<sup>NICD</sup>* mice, suggesting compensation by a Notch  
37 signaling pathway other than Hes1. Conversely, *Pdx1-Cre;Hes1<sup>ff</sup>* mice showed impaired postnatal  
38 exocrine development in both the pancreatic head and tail, revealing that the timing and  
39 distribution of embryonic Hes1 expression affects postnatal exocrine tissue development.

40 *Conclusions* Notch signaling has an essential role in pancreatic progenitor cells for the postnatal  
41 maturation of exocrine tissue, partly through the formation of centroacinar cells.

42

43

44 **Key words:**

45 Hes1, Notch signaling, pancreas, postnatal development, centroacinar cell

46

47

## 48 **Introduction**

49 The pancreas consists of both exocrine and endocrine tissues. During embryonal development,  
50 these exocrine or endocrine cells are known to differentiate from common pancreatic progenitor  
51 cells that are positive for Pdx1 or Ptf1a [1]. Ptf1a is coexpressed with Pdx1 in the pancreatic  
52 epithelia at embryonic day 9.0. Pdx1 is expressed as early as embryonic day 8.5 not only in the  
53 pancreas but also in the duodenum, bile duct, and posterior part of the stomach [2]. Notch signaling  
54 plays an important role in the development and maintenance of these progenitor cells, in addition  
55 to determining their cell fate [3]. However, the detailed functions of Notch signaling after  
56 exocrine/endocrine determination or during postnatal pancreatic maturation have not been fully  
57 elucidated.

58 Notch signaling is triggered when ligands interact with Notch receptors. The Notch intracellular  
59 domain (NICD) then translocates to the nucleus and activates target genes such as *Hes1*, a main  
60 target of the signaling [3]. During pancreatic development, systemic *Hes1*-deficient mice have  
61 accelerated endocrine cell differentiation of pancreatic progenitor cells via upregulation of *Ngn3*,  
62 a master gene of endocrine differentiation. This leads to reduction of progenitor cells and  
63 pancreatic hypoplasia [4]. *Hes1*-deficient mice are also reported to have induced ectopic  
64 expression of Ptf1a and subsequently form ectopic pancreatic tissue [5]. From these observations,  
65 Notch/*Hes1* signaling is thought to play a critical role in the development, maintenance, and cell  
66 fate determination of pancreatic progenitors by regulating downstream molecules, including Ptf1a  
67 and *Ngn3*. In contrast to these functions at embryonic day 8.5–9.0, Notch signaling also plays a  
68 role after Pdx1 or Ptf1a expression. In mice that have conditional NICD expression in Pdx1-  
69 expressing cells, pancreatic progenitor cell differentiation was inhibited [6]. Conversely, mice that  
70 have *Hes1* conditionally knocked out in Ptf1a-expressing cells revealed no apparent phenotype at  
71 birth, although pancreatic atrophy and fatty metaplasia were observed in adults [7]. Thus, the role

72 of Notch signaling in pancreatic cells after embryonic Pdx1 or Ptf1a expression is still  
73 controversial.

74 Rather than embryonic Pdx1-positive and Ptf1a-positive progenitor cells, centroacinar cells are  
75 considered one of the candidates for adult pancreatic tissue stem cells. Centroacinar cells are  
76 located at the junction between peripheral acinar cells and the adjacent ductal epithelium, and are  
77 characterized by high levels of ALDH1 enzymatic activity and marked Sca1, Sdf1, c-Met, Nestin,  
78 and Sox9 expression. These are markers that have been previously associated with progenitor  
79 populations in the embryonic pancreas and other tissues [8]. Cre-based lineage tracing showed that  
80 adult Sox9-positive duct and/or centroacinar cells continuously supplied acinar cells, suggesting  
81 that centroacinar cells have characteristics of stem cells [9]. Interestingly, Hes1 was reported to be  
82 expressed in centroacinar cells [10], and the abrogation of both Notch receptor ligands, Delta-like  
83 1 and Jagged1, led to the loss of centroacinar cells [11]. These observations suggest that Notch  
84 signaling is highly related to centroacinar cell formation.

85 In the current study, to elucidate the role of Notch signaling in Pdx1-positive or Ptf1a-positive  
86 pancreatic progenitor cells, we analyzed the phenotype of mice with *Hes1* gene knockout and/or  
87 NICD transgenic expression in Pdx1- or Ptf1a-expressing cells. We found that in pancreatic  
88 progenitor cells, Notch signaling plays an essential role in postnatal exocrine tissue development,  
89 presumably in part via centroacinar cell formation.

90

## 91 **Methods**

### 92 **Mice**

93 Experimental animals were generated by crossing *Ptf1a<sup>cre/+</sup>* [1] or *Pdx1-Cre* [12] (supplied by Y  
94 Kawaguchi, Kyoto University, Kyoto, Japan) with *Hes1<sup>ff</sup>* [13] and/or *Rosa26<sup>NICD</sup>* [6] (supplied by  
95 D Melton, Harvard University, MA, USA). To examine Cre expression in the pancreas, we crossed

96 these mice with *Rosa26<sup>LacZ</sup>* mice. Each mouse strain is shown in Supplementary Figure 1. All mice  
97 were maintained on a mixed genetic background. To compare the phenotypes of genetically  
98 engineered mice and controls, we used 3 to 7 littermate mice from each group and age group. No  
99 selection for a specific sex was performed in this study except for body weight. All animal  
100 experiments were approved by the Kyoto University Graduate School and Faculty of Medicine  
101 Ethics Committee.

102

### 103 **Histological study**

104 For histological studies, tissue samples were excised from the mice, flushed with phosphate-  
105 buffered saline (PBS), fixed overnight in 10% neutral phosphate-buffered formalin, and embedded  
106 in paraffin. Sections of 5- $\mu$ m thickness were stained with H&E, and immunohistochemistry was  
107 carried out. Tissue samples were also frozen immediately in liquid nitrogen for X-gal staining and  
108 immunofluorescence studies. Bright-field and fluorescence images were captured with an  
109 Olympus BX53-33FL microscope (Olympus, Tokyo, Japan) or Keyence BZ-X710 microscope  
110 (Keyence, Osaka, Japan). The captured images were analyzed with Adobe Photoshop software.

111

### 112 **Immunohistochemistry and immunofluorescence**

113 Immunohistochemical study was performed using a standard method as previously reported [14].  
114 Primary antibodies used in this study are listed in Supplementary Table 1. Staining signals were  
115 detected using a Vectorstain Elite ABC Kit (Vector Laboratories, Burlingame, CA) and a  
116 peroxidase substrate kit, DAB (Vector Laboratories). The peroxidase reaction was carried out with  
117 Liquid DAB+ Substrate Chromogen System (Dako). Finally, slides were counterstained with  
118 hematoxylin (Wako, Japan).

119 For immunofluorescence studies, the primary antibodies listed in Supplementary Table 1 were

120 used. The secondary antibodies were Alexa Fluor 594 anti-rabbit IgG 1:100 (A-21207, Thermo  
121 Fisher Scientific, Waltham, MA, USA), Alexa Fluor 488 anti-mouse IgG 1:100 (A-21200, Thermo  
122 Fisher Scientific), Dylight 488 anti-guinea pig IgG 1:100 (ab96959, Abcam plc, Cambridge, UK),  
123 and Alexa Fluor 488 anti-rabbit IgG 1:100 (A-11008, Thermo Fisher Scientific). To assess co-  
124 localization of Hes1 and Aldh1a1, frozen sections were stained with anti-Hes1 antibody with Alexa  
125 Fluor 594 (ab207048, Abcam) and anti-Aldh1a1 with Alexa Fluor 488 (ab195254, abcam).

126

### 127 **X-gal staining**

128 We performed X-gal staining as previously described [1]. Briefly, freshly isolated pancreas was  
129 incubated in ice-cold fixative solution (PBS containing 4% paraformaldehyde, 5 mmol/L EGTA,  
130 2 mmol/L MgCl<sub>2</sub>, 0.2% glutaraldehyde, and 0.02% NP-40) for 1 hour at 4 °C. After washing twice  
131 in PBS for 20 minutes, tissues were incubated with LacZ substrate (PBS containing 5 mmol/L  
132 K<sub>3</sub>Fe(CN)<sub>6</sub>, 5 mmol/L K<sub>4</sub>Fe(CN)<sub>6</sub>, 2 mmol/L MgCl<sub>2</sub>, 0.02% NP-40, 0.1% sodium deoxycholate,  
133 and 1 mg/mL X-galactosidase) overnight at room temperature. After washing twice in PBS for 20  
134 minutes, tissues were fixed overnight in 4% paraformaldehyde in PBS at 4 °C. Paraformaldehyde  
135 was removed, and the stained tissues were transferred to tissue cassettes.

136

### 137 **Evaluation of Ki67-positive cells, cleaved caspase3-positive cells, and centroacinar cells**

138 We compared the number of Ki67-positive cells and cleaved caspase3-positive cells between  
139 *Ptfla<sup>cre/+</sup>;Hes1<sup>ff</sup>* mice and control mice at P0. To count Ki67-positive cells, we used two fields of  
140 200-fold magnification randomly selected in both the head and tail of the pancreas. For cleaved  
141 caspase3-positive cells, we counted all positive cells in both the head and tail of the pancreas in a  
142 whole slice. We measured the area of the pancreas using ImageJ (<http://imagej.nih.gov/ij/>). To  
143 compare the ratio of acini without centroacinar cells, we counted the number of acini with vacant

144 space in the center of acini and the number of normal acini in *Ptfla<sup>cre/+</sup>;Hes1<sup>ff</sup>* mice and control  
145 mice at P0.

146

### 147 **Western blot analysis**

148 To evaluate autophagy in the pancreatic tissue, we performed Western blot analysis for LC3-I and  
149 its lipidated form LC3-II, which are widely used to quantify autophagy [15]. Protein extracts from  
150 both pancreatic tissue of *Ptfla<sup>cre/+</sup>;Hes1<sup>ff</sup>* mice and control mice at P4 were boiled in Laemmli  
151 sample buffer with 2.5% mercaptoethanol, fractionated on 4–15% sodium dodecyl sulfate  
152 polyacrylamide gels (456-1806, Bio-Rad, Tokyo, Japan), and transferred to nitrocellulose  
153 membranes according to standard protocols. After blocking with 5% dry skim milk, the blots were  
154 incubated with primary antibodies. The primary antibodies were anti-LC3 (1:1000; PM036, MBL,  
155 Japan) and anti-β actin (1:10000; ab6276, Abcam). The secondary antibodies were peroxidase-  
156 conjugated anti-mouse IgG (1:4000; NA931, GE Healthcare, Chicago, IL, USA) or anti-rabbit IgG  
157 (1:10 000; 31458, Thermo Fisher Scientific).

158

### 159 **Microarray analysis**

160 We sacrificed a *Ptfla<sup>cre/+</sup>;Hes1<sup>ff</sup>* mouse and a control mouse (*Ptfla<sup>cre/+</sup>; Hes1<sup>+/+</sup>*) at postnatal day  
161 7 and collected pancreatic head and tail tissues from each mouse. Total RNA was extracted from  
162 the pancreatic tissue collected in RNALater (Ambion) using RNeasy kit (QIAGEN, Hilden,  
163 Germany) according to the manufacturer's instructions. RNA Integrity Number (RIN) of extracted  
164 RNA from pancreatic head of control mouse, tail of a control mouse, head of a *Ptfla<sup>cre/+</sup>;Hes1<sup>ff</sup>*  
165 mouse, and tail of a *Ptfla<sup>cre/+</sup>;Hes1<sup>ff</sup>* mouse were 9.2, 9.5, 9.2, and 9.1, respectively. RNA was  
166 analyzed by Agilent's microarray.

167 We determined genes associated with pancreatic development, which were specified in a review



168 article [16]. We then selected genes whose expression in the *Ptfla<sup>cre/+</sup>;Hes1<sup>fl/fl</sup>* mouse were more  
169 than twice or less than half of that of the control. We analyzed these genes and constructed  
170 heatmaps with R (R Core Team (2016). R: A language and environment for statistical computing.  
171 R Foundation for Statistical Computing, Vienna, Austria. URL <https://www.R-project.org/>.)

172

### 173 **Quantitative RT-PCR**

174 Total RNA was extracted from the pancreatic tissue collected in RNALater (Ambion) using  
175 RNeasy kit (QIAGEN, Hilden, Germany), according to the manufacturer's instructions. For  
176 complementary DNA synthesis, 1 µg total RNA was reverse transcribed using ReverTra Ace<sup>®</sup>  
177 qPCR RT Master Mix (Toyobo, Osaka, Japan) and subjected to quantitative RT-PCR. Quantitative  
178 RT-PCR was performed by using the LightCycler<sup>®</sup> system (Roche, Switzerland). The mRNA  
179 expression of specific genes was measured using FastStart Universal SYBR Green Master (Roche,  
180 Switzerland). RNA levels were normalized to the level of the housekeeping gene GAPDH and  
181 calculated as delta-delta threshold cycle ( $\Delta\Delta CT$ ). The primer sequences used for mouse ALDH1A1  
182 and GAPDH were as follows: mouse ALDH1A1, 5'-GGGCTGACAAGATTCATGGT-3'  
183 (forward) and 5'-GGAAAATTCCAGGGGATGAT-3' (reverse); and GAPDH, 5'-  
184 AGGTCGGTGTGAACGGATTTG-3' (forward) and 5'- TGTAGACCATGTAGTTGAGGTCA -  
185 3' (reverse). All quantitative RT-PCR analyses were performed in triplicate.

186

### 187 **FACS isolation of Aldh-positive cells**

188 FACS isolation of Aldh-positive cell was performed using just modified previously described  
189 method [17]. Pancreas of *Ptfla<sup>cre/+</sup>;Hes1<sup>fl/fl</sup>* mice and control mice were dissected at P7, washed in  
190 iced HBSS solution (Thermo Fisher Scientific, Waltham, MA, USA) and minced into small pieces.  
191 The minced pancreas was digested by 1 mg/ml collagenase D (Roche, Switzerland) dissolved in

192 DMEM (Gibco) and supplemented with 2 U/ml DNase I (Promega, Madison, WI, USA) and 1%  
193 BSA (Wako) for twenty minutes on a shaker at 37°C. Cells were pipetted through a 1 mL pipette  
194 tip every 5 minutes. The reaction was stopped by adding ice cold DMEM supplemented with 5%  
195 FBS. Cells were then passed through a 100, 70, and 40 µm cell strainer sequentially, centrifuged  
196 at 300 g, 4°C for 3 minutes, re-suspended with DMEM, and counted. Cell suspension were treated  
197 with Aldefluor reagent (Stem Cell Technologies, Vancouver, Canada) in the dark at 37 °C on a  
198 shaker for 30 minutes. Diethylaminobenzaldehyde (DEAB), an inhibitor of Aldh activity was also  
199 added for negative control. Following the Aldefluor reaction, cells were centrifuged and re-  
200 suspended with DMEM. FACS Aria II (BD, Franklin Lakes, NJ, USA) was used for FACS sorting.  
201 FSC and SSC were used for exclusion of cell debris. Aldh-positive cells were isolated by Aldefluor  
202 activity (FITC channel) and counted.

203

### 204 **Three-dimensional organoid culture of adult pancreatic cells**

205 Cells re-suspended with DMEM as described above were seeded in 25 µL of the growth factor-  
206 reduced Matrigel (BD) in a 48-well plate (Corning). In each well, 1000 cells were seeded. After  
207 the gelation of the Matrigel for 10 minutes at 37°C in the incubator, culture medium was added.  
208 Culture medium was based on AdDMEM/F12 (Thermo Fischer Scientific), supplemented with 2%  
209 B27 (Thermo Fischer Scientific), 1% penicillin/streptomycin (Thermo Fischer Scientific), 1 mM  
210 HEPES (Thermo Fischer Scientific), 1% Glutamax (Thermo Fischer Scientific), 1.25 mM N-  
211 Acetylcysteine (Sigma), 10 nM gastrin (Sigma), 50 ng/ml EGF (Peprotech), 250 ng/ml Rspodin1  
212 (R&D Systems), 100 ng/ml Noggin (Peprotech), 100 ng/ml FGF10 (Peprotech), 10 mM  
213 Nicotinamide (Sigma), 500 nM A83-01 (Tocris), and 10 µM Y27632 (Tocris Bioscience). Culture  
214 medium was changed every 3 days. The number and size of organoids were counted 5 days and 9  
215 days after seeding.

216

## 217 **Statistical analysis**

218 Data are expressed as the median and standard error of the mean. Statistical comparisons were  
219 calculated using an unpaired two-tailed Student's t-test for continuous data. A p-value of less than  
220 0.05 was considered to indicate significance.

221

222

## 223 **Results**

### 224 ***Hes1* knockout in *Ptf1a*-positive progenitor cells does not affect fetal pancreatic development**

225 To elucidate the role of *Hes1* in *Ptf1a*-positive progenitor cells during pancreatic development,  
226 we generated conditional *Hes1* knockout mice by crossing *Ptf1a-Cre* mice (*Ptf1a<sup>cre/+</sup>*) [1], *Hes1*  
227 floxed mice (*Hes1<sup>fl/fl</sup>*) [13], and *Rosa26<sup>LacZ</sup>* mice (Fig. S1a-c). Conditional *Hes1* knockout (*Hes1*  
228 *cKO*, *Ptf1a<sup>cre/+</sup>;Hes1<sup>fl/fl</sup>;Rosa26<sup>LacZ</sup>*) mice were born at expected Mendelian ratio, and successful  
229 *Hes1* deletion was confirmed by immunohistochemistry (Fig. S2). First, we analyzed neonatal  
230 mice. As a result, there was no macroscopic difference in pancreatic size between *Hes1 cKO* and  
231 control (*Ptf1a<sup>+/+</sup>;Hes1<sup>fl/fl</sup>;Rosa26<sup>LacZ</sup>*, *Ptf1a<sup>cre/+</sup>;Hes1<sup>+/+</sup>;Rosa26<sup>LacZ</sup>* or  
232 *Ptf1a<sup>cre/+</sup>;Hes1<sup>fl/+</sup>;Rosa26<sup>LacZ</sup>*) mice at P0 (Fig. 1a). This was also clearly demonstrated by X-gal  
233 staining (Fig. 1a). There was also no difference in body weight and blood glucose levels between  
234 *Hes1 cKO* and control mice at 1 week of age (Fig. S3). Microscopically, hematoxylin and eosin  
235 (H&E) staining revealed normal pancreatic acini, ducts, and islets of Langerhans in *Hes1 cKO*  
236 mice (Fig. 1a). Furthermore, there was no difference between *Hes1 cKO* and control mice when  
237 evaluating acinar cells, duct cells,  $\beta$  cells, and  $\alpha$  cells via immunohistochemistry for amylase,  
238 cytokeratin, insulin, and glucagon, respectively (Fig. 1b). Thus, no obvious abnormality was  
239 detected in *Ptf1a<sup>cre/+</sup>;Hes1<sup>fl/fl</sup>;Rosa26<sup>LacZ</sup>* mice at P0.

240

241 **Transgenic Notch1 expression in Ptf1a-positive progenitor cells does not affect fetal**  
242 **pancreatic development**

243 To further analyze the role of Notch signaling in Ptf1a-positive progenitor cells in pancreatic  
244 development, we next generated *Ptf1a<sup>cre/+</sup>;Rosa26<sup>NICD</sup>* mice (Fig. S1d) [6]. In these mice,  
245 transgenic expression of the Notch1 intracellular domain activates downstream molecules of Notch  
246 signaling, including Hes1. As a result, there were no macroscopic differences in pancreatic size  
247 between *Ptf1a<sup>cre/+</sup>;Rosa26<sup>NICD</sup>* and control (*Ptf1a<sup>+/+</sup>; Rosa26<sup>NICD</sup>*) mice (Fig. 2a) at P0.  
248 Microscopically, there was no difference in the development of exocrine and endocrine tissues  
249 between *Ptf1a<sup>cre/+</sup>;Rosa26<sup>NICD</sup>* and control mice at P0 (Fig. 2a), whereas some acinar cells showed  
250 ductal change in part (Fig. 2b). Immunofluorescent staining showed normal number of amylase-  
251 positive acinar cells, cytokeratin-positive duct cells (Fig. 2b), insulin-positive  $\beta$  cells, and  
252 glucagon-positive  $\alpha$  cells (Fig. 2c) in *Ptf1a<sup>cre/+</sup>;Rosa26<sup>NICD</sup>* mice as compared to control mice.  
253 These results indicated that both *Hes1* knockout and *Notch1* overexpression in Ptf1a-positive  
254 progenitor cells do not affect the fetal development of pancreatic tissue.

255

256 ***Hes1* knockout in Ptf1a-positive progenitor cells results in exocrine atrophy of the adult**  
257 **pancreatic tail**

258 As shown above, *Hes1 cKO* (*Ptf1a<sup>cre/+</sup>;Hes1<sup>fl/fl</sup>;Rosa26<sup>LacZ</sup>*) mice showed normal pancreatic  
259 development at birth. After birth, there was no difference in body weight and glucose levels  
260 between *Hes1 cKO* and control mice (Fig. S3). However, detailed time-course analysis by X-gal  
261 staining revealed that the pancreatic tail gradually showed atrophic changes, and was replaced by  
262 fat tissue by 4 weeks of age (Fig. 3a, Fig. S4). Meanwhile, the pancreas head was not affected by  
263 fat replacement. Histological analysis by H&E staining and immunohistochemistry was performed

264 at 4 weeks of age for amylase and cytokeratin. This confirmed remarkable loss of acinar cells,  
265 abnormal alignment of duct cells, and prominent deposition of fat tissue in the pancreatic tail of  
266 *Hes1 cKO* mice compared to that of control mice or the pancreatic head of *Hes1 cKO* mice (Fig.  
267 3b). In contrast to the marked impairment of exocrine cells, normal endocrine cell development  
268 was observed in both the pancreatic head and tail of *Hes1 cKO* mice when analyzed via  
269 immunohistochemistry for insulin and glucagon (Fig. 3b).

270 To investigate the cause of atrophic changes in the pancreatic tail of *Hes1 cKO* mice, apoptosis  
271 and cell growth levels were evaluated by immunohistochemistry for cleaved caspase3 and Ki67,  
272 respectively, at age P0 (Fig. 4a). Although there was no difference in histology (Fig. 1) and the  
273 Ki67 index (Fig. 4b) between *Hes1 cKO* and control mice in both the pancreatic head and tail,  
274 significantly more apoptotic cells were detected in *Hes1 cKO* than in control mice, especially in  
275 the pancreatic tail (Fig 4c). Western blot analysis revealed expression of LC3- I , but failed to  
276 detect its lipidated form LC3- II in both pancreatic head and tail of *Hes1 cKO* mice and control  
277 mice (Fig. S5), suggesting a limited involvement of autophagy. These results showed that  
278 conditional *Hes1* knockout in *Ptf1a*-positive progenitor cells led to atrophic changes in the  
279 pancreatic tail during the postnatal growth and maturation process, partly due to exocrine cell  
280 apoptosis.

281

### 282 ***Hes1* knockout in *Ptf1a*-positive progenitor cells induces centroacinar cell reduction**

283 To further investigate the cause of atrophic changes in the pancreatic tail of *Hes1 cKO* mice, we  
284 focused on centroacinar cells located in the center of the pancreatic acinus. These are considered  
285 to be one of the adult tissue stem cell candidates of pancreatic exocrine tissue. As previously  
286 reported, centroacinar cells with *Hes1* and *Aldh1* expression were observed in the pancreatic tail

287 of control (*Ptf1a<sup>cre/+</sup>;Hes1<sup>f/+</sup>*) mice at P0 (Fig 5a). Co-localization of Hes1 and Aldh1a1 was  
288 confirmed by immunofluorescence at P3 (Fig. S6a). In contrast, in *Hes1 cKO* (*Ptf1a<sup>cre/+</sup>;Hes1<sup>f/f</sup>*)  
289 mice, there were a substantial number of acini with vacant space in the center and without Hes1-  
290 and Aldh1-positive centroacinar cells (Fig 5a). The ratio of acini without centroacinar cells was  
291 significantly higher in the pancreatic head and tail of *Hes1 cKO* mice than in control mice at P0  
292 (Fig 5b). At P3, this trend of centroacinar cell reduction was prolonged in the pancreatic tail,  
293 whereas this trend was disappeared in pancreatic head (Fig 5c). At P7, microarray analysis using  
294 tissue from the pancreatic tail of *Hes1 cKO* mice revealed distinct gene expression patterns from  
295 that of the pancreatic head of *Hes1 cKO* mice or the pancreatic head/tail of control mice (Fig. S6b).  
296 Notably, the pancreatic tail of *Hes1 cKO* mice showed decreased exocrine-related gene expression  
297 (Fig. 5d) and increased endocrine-related gene expression (Fig. 5e). Lower *Aldh1*-related gene  
298 expression and significantly reduced *Aldh1a1* gene expression were demonstrated by microarray  
299 (Fig. 5f) and qPCR analysis (Fig. 5g), respectively, in the pancreatic tail of *Hes1 cKO* mice  
300 compared to that of control mice. This confirmed the previously observed reduction in centroacinar  
301 cells in the pancreatic tail of *Hes1 cKO* mice (Fig. 5a-c). The presence of fewer centroacinar cells  
302 in the pancreatic tail of *Hes1 cKO* mice in the neonatal state may explain pancreatic atrophy being  
303 observed only in the pancreatic tail.

304 To further assess the mechanisms for fewer centroacinar cells and subsequent impaired  
305 development in *Hes1 cKO* mice, we isolated pancreatic cells from *Hes1 cKO* and control mice and  
306 evaluated their stem cell features by FACS analysis and organoid culture. As a result, confirming  
307 the altered *Aldh1*-related gene expression (Fig. 5f), FACS analysis revealed that pancreatic tail of  
308 *Hes1 cKO* mice had significantly lower number of Aldh-positive cells than control mice at P7 (Fig.  
309 S7a, b). Furthermore, pancreatic cells from *Hes1 cKO* mice formed significantly lower number of  
310 organoids than those from control mice (Fig. S7c, d). These observations suggest that loss of Hes1

311 may affect the maintenance of tissue stem cells required for postnatal pancreatic development.

312

313 **Transgenic *Notch1* expression compensates for the *Hes1* knockout phenotype in *Ptf1a*-**  
314 **positive progenitor cells**

315 To assess the role of the Notch signaling pathway in postnatal pancreatic tail development, we  
316 analyzed *Ptf1a<sup>cre/+</sup>;Hes1<sup>ff</sup>;Rosa26<sup>NICD</sup>* mice. In these mice, downstream molecules of Notch  
317 signaling, other than *Hes1*, were activated in *Ptf1a*-positive progenitor cells. As a result, some acini  
318 showed a vacant space without centroacinar cells in *Ptf1a<sup>cre/+</sup>;Hes1<sup>ff</sup>;Rosa26<sup>NICD</sup>* mice at P0 (Fig.  
319 6a), as observed in *Ptf1a<sup>cre/+</sup>;Hes1<sup>ff</sup>* mice (Fig. 5a). However, even with *Hes1* gene deletion,  
320 atrophic changes in the pancreatic tail were not observed in *Ptf1a<sup>cre/+</sup>;Hes1<sup>ff</sup>;Rosa26<sup>NICD</sup>* mice at  
321 16 weeks of age. H&E staining, immunohistochemistry for amylase and cytokeratin, and  
322 immunofluorescence staining for insulin and glucagon showed normal development of acinar cells,  
323 duct cells,  $\alpha$  cells, and  $\beta$  cells in *Ptf1a<sup>cre/+</sup>;Hes1<sup>ff</sup>;Rosa26<sup>NICD</sup>* mice at 16 weeks (Fig. 6b,c).  
324 These results suggested that activation of the Notch signaling pathway, other than *Hes1*, could  
325 compensate for defective *Hes1* in pancreatic tail development in the postnatal to adult state. To  
326 further analyze this compensatory mechanism, we assessed the expressions of *Hes5* and *Hey1*,  
327 which are major downstream molecules of Notch signaling other than *Hes1*, in pancreatic tissues  
328 of *Ptf1a<sup>cre/+</sup>;Hes1<sup>ff</sup>;Rosa26<sup>NICD</sup>* mice, *Ptf1a<sup>cre/+</sup>;Rosa26<sup>NICD</sup>* mice, *Ptf1a<sup>cre/+</sup>;Hes1<sup>ff</sup>* (*cKO*) mice,  
329 and control mice at P0 by immunohistochemistry. As a result, a marked increase of *Hes5*  
330 expression was observed in *Ptf1a<sup>cre/+</sup>;Hes1<sup>ff</sup>;Rosa26<sup>NICD</sup>* mice compared to *Ptf1a<sup>cre/+</sup>;Rosa26<sup>NICD</sup>*  
331 mice, *Ptf1a<sup>cre/+</sup>;Hes1<sup>ff</sup>* (*cKO*) mice and control mice, whereas *Hey1* expression was similar in all  
332 the strains of mice (Fig. S8). These results suggested that *Hes5* could be one of the factors  
333 contributing the compensation for *Hes1* deficiency in pancreatic development in  
334 *Ptf1a<sup>cre/+</sup>;Hes1<sup>ff</sup>;Rosa26<sup>NICD</sup>* mice.

335

336 ***Hes1* knockout in Pdx1-positive progenitor cells induces impaired exocrine development in**  
337 **both the pancreatic head and tail**

338 We sought to investigate why the pancreatic head did not have impaired exocrine development  
339 in mice with conditional *Hes1* knockout in Ptf1a-positive progenitor cells  
340 (*Ptf1a<sup>cre/+</sup>;Hes1<sup>fl/fl</sup>;Rosa26<sup>LacZ</sup>*). To this end, we generated and analyzed *Pdx1-*  
341 *Cre;Hes1<sup>fl/fl</sup>;Rosa26<sup>LacZ</sup>* mice, in which *Hes1* gene is expected to be knocked out in pancreatic  
342 progenitor cells by Pdx1-Cre [12] (Fig. S1e) about 0.5 day prior to that by Ptf1a-Cre. Similar to  
343 *Ptf1a<sup>cre/+</sup>;Hes1<sup>fl/fl</sup>* mice, normal exocrine/endocrine cells and a substantial number of acini without  
344 centroacinar cells were observed in *Pdx1-Cre;Hes1<sup>fl/fl</sup>;Rosa26<sup>LacZ</sup>* mice via H&E staining and  
345 immunofluorescent staining for insulin and glucagon at P0 (Fig. 7a,b). X-gal staining of *Pdx1-*  
346 *Cre;Hes1<sup>fl/fl</sup>;Rosa26<sup>LacZ</sup>* mice stained almost all pancreatic cells blue at P0, suggesting that *Hes1*  
347 was successfully knocked out in these cells (Fig. 7c). In contrast, at 2 weeks and 54 weeks after  
348 birth, although the size of the pancreas was normal, the number of blue cells stained by X-gal  
349 staining was markedly reduced in both the pancreatic head and tail in *Pdx1-Cre;Hes1<sup>fl/fl</sup>;Rosa26<sup>LacZ</sup>*  
350 mice as compared to that in control mice (Fig. 7c). In the microscopic analysis of X-gal staining,  
351 while all the pancreatic cells were stained blue at P0, only endocrine cells and a few exocrine cells  
352 were stained blue in *Pdx1-Cre;Hes1<sup>fl/fl</sup>;Rosa26<sup>LacZ</sup>* mice at 8 weeks of age. Further, pancreatic tissue  
353 replaced non-stained exocrine cells in both the pancreatic head and tail at 8 weeks of age (Fig. 7d).  
354 These results indicated that *Hes1*-knocked out Pdx1-positive progenitor cells could not mature into  
355 exocrine cells in the pancreatic head or tail. This is different from the observations found in *Hes1-*  
356 knocked out Ptf1a-positive progenitor cells. The results suggest that the timing of *Hes1* expression  
357 in the embryonic stage critically affects the postnatal development of exocrine tissue.

358



359

## 360 **Discussion**

361 The importance of Notch signaling in pancreatic embryonic development has been thoroughly  
362 studied [3, 4]. However, since systemic *Hes1* deficient mice or *Pdx1-Cre;Rosa26<sup>NICD</sup>* mice are  
363 reported to be embryonic lethal mutants [4, 6] the detailed functions of Notch signaling in Pdx1-  
364 or Ptf1a-positive progenitor cells has been mostly unknown. In this study, we analyzed mice with  
365 conditional *Hes1* knockout or transgenic NICD expression in Ptf1a/Pdx1-positive progenitor cells.  
366 We found that Notch signaling in pancreatic progenitor cells plays an essential role in postnatal  
367 exocrine tissue development.

368 Previous reports have shown that systemic *Hes1* knockout induced accelerated differentiation of  
369 pancreatic progenitor cells to endocrine cells, resulting in a reduction in progenitor cells. This  
370 suggests the crucial role of Notch/Hes1 signaling in exocrine-endocrine cell fate determination [4].  
371 This function of Notch signaling is still observed in Pdx1-positive progenitor cells, in which  
372 exocrine-endocrine differentiation was inhibited by conditional NICD expression [6]. However, in  
373 our analysis, both *Ptf1a<sup>cre/+</sup>;Hes1<sup>ff</sup>* mice and *Ptf1a<sup>cre/+</sup>;Rosa26<sup>NICD</sup>* mice showed normal  
374 embryonic development, and no abnormality was observed in exocrine-endocrine differentiation  
375 at birth. Considering that gene recombination is induced in pancreatic progenitor cells by Pdx1-  
376 Cre at about 0.5 to 1 day prior to that by Ptf1a-Cre [2], cell fate determination by Notch signaling  
377 may have already been completed in Ptf1a-positive pancreatic progenitor cells.

378 In contrast, our analysis showed that *Ptf1a<sup>cre/+</sup>;Hes1<sup>ff</sup>* mice had atrophic changes in the pancreatic  
379 tail by 4 weeks of age due to impaired postnatal development exocrine tissue. This is similar to the  
380 observations details in the report by Hidalgo-Sastre et al. [7], From these observations, it is clear  
381 that *Hes1* plays a critical role in exocrine tissue maturation after exocrine cell fate determination  
382 in Ptf1a-positive progenitor cells. To elucidate the mechanism of impaired postnatal pancreatic

383 exocrine tissue development in *Ptfla<sup>cre/+</sup>;Hes1<sup>ff</sup>* mice, we focused on centroacinar cells. These  
384 cells are one of the candidates for adult pancreatic tissue stem cells, and have been reported to  
385 express Hes1 [10]. As a result, we found sustained loss of centroacinar cells during the neonatal  
386 period in the pancreatic tail, but not in the pancreatic head, in *Ptfla<sup>cre/+</sup>;Hes1<sup>ff</sup>* mice. This  
387 phenotype of centroacinar cell loss and acini with vacant space in the center is markedly analogous  
388 to that of Notch ligands *Dll1/Jag1* double knockout mice [11], suggesting the role of Notch  
389 signaling in centroacinar cell development. Together with our results of increased apoptotic cells  
390 in the pancreatic tail of *Ptfla<sup>cre/+</sup>;Hes1<sup>ff</sup>* mice, Notch signaling in pancreatic progenitor cells may  
391 contribute to postnatal centroacinar cell development and subsequent exocrine maturation. To  
392 confirm this hypothesis, we analyzed *Ptfla<sup>cre/+</sup>;Hes1<sup>ff</sup>;Rosa26<sup>NICD</sup>* mice in which Notch signaling,  
393 save for Hes1, is activated. As expected, the impaired postnatal pancreatic exocrine tissue  
394 development in *Ptfla<sup>cre/+</sup>;Hes1<sup>ff</sup>* mice was completely rescued by the activation of Notch signaling  
395 in *Ptfla<sup>cre/+</sup>;Hes1<sup>ff</sup>;Rosa26<sup>NICD</sup>* mice, suggesting that *Hes/Hey* family members other than *Hes1*  
396 may have compensated for the function of *Hes1*. In fact, expression of Hes5 was strongly enhanced  
397 in the pancreatic tissue of *Ptfla<sup>cre/+</sup>;Hes1<sup>ff</sup>;Rosa26<sup>NICD</sup>* mice, suggesting that Hes5 may contribute  
398 to this compensatory mechanism.

399 We sought to determine when Notch/Hes1 signaling carries out its critical function in postnatal  
400 pancreatic progenitor cell maturation after performing its role in exocrine/endocrine cell fate  
401 determination at the embryonic stage. We, therefore, analyzed *Pdx1-Cre;Hes1<sup>ff</sup>* mice in  
402 comparison with *Ptfla<sup>cre/+</sup>;Hes1<sup>ff</sup>* mice. As a result, impaired postnatal exocrine maturation was  
403 observed only in the pancreatic tail in *Ptfla<sup>cre/+</sup>;Hes1<sup>ff</sup>* mice. However, this was observed in both  
404 the pancreatic head and tail in *Pdx1-Cre;Hes1<sup>ff</sup>* mice. We speculate that this phenotypic difference  
405 in the pancreatic head between *Ptfla<sup>cre/+</sup>* and *Pdx1-Cre* is due to their difference in timing of  
406 genetic recombination, as mentioned above [2]. The appearance of this phenotype in *Pdx1-Cre* but

407 not in *Ptfla<sup>cre/+</sup>* may indicate the importance of Notch signaling activation between Pdx1 and *Ptfla*  
408 expression in progenitor cells, at least in the pancreatic head. The greater effect by earlier *Hes1*  
409 deletion is further confirmed by our previous observation that adult pancreatic tissue is resistant to  
410 *Hes1* deletion [14]. Interestingly, unlike *Ptfla<sup>cre/+</sup>;Hes1<sup>ff</sup>* mice, pancreatic atrophy was not  
411 observed in *Pdx1-Cre;Hes1<sup>ff</sup>* mice. This is probably because the loss of X-gal positive / *Hes1*  
412 knockout cells was replaced by X-gal negative exocrine cells that escaped the recombination of  
413 *Hes1* gene.

414 In conclusion, in addition to the previously reported role of exocrine/endocrine cell fate  
415 determination, Notch signaling in pancreatic progenitor cells plays an essential role in the postnatal  
416 maturation of exocrine tissue, partly through centroacinar cell formation.

417

418

419 **Acknowledgements**

420 We thank Y Kawaguchi (Kyoto University, Kyoto, Japan) for supplying *Ptfla<sup>cre/+</sup>* mice. We thank  
421 D Melton (Harvard University, MA, USA) for supplying *Rosa26<sup>NICD</sup>* mice. We thank Yuta  
422 Kawamata and Taichi Ito for the excellent technical support.

423

424 **Funding**

425 This work was supported by the Japan Society for the Promotion of Science (JSPS) KAKENHI  
426 Grant Numbers JP16K09395.

427

428 **Competing interests**

429 The authors declare that they have no conflict of interest.

430

431

432 **References**

- 433 1. Kawaguchi Y, Cooper B, Gannon M, et al. The role of the transcriptional regulator Ptf1a in  
434 converting intestinal to pancreatic progenitors. *Nat Genet.* 2002;32:128-134.
- 435 2. Jørgensen MC, Ahnfelt-Rønne J, Hald J, et al. An illustrated review of early pancreas  
436 development in the mouse. *Endocr Rev.* 2007;28:685-705.
- 437 3. Kageyama R, Ohtsuka T, Kobayashi T. The Hes gene family: repressors and oscillators that  
438 orchestrate embryogenesis. *Development.* 2007;134:1243-1251.
- 439 4. Jensen J, Pedersen EE, Galante P, et al. Control of endodermal endocrine development by Hes-  
440 1. *Nat Genet.* 2000;24:36-44.
- 441 5. Fukuda A, Kawaguchi Y, Furuyama K, et al. Ectopic pancreas formation in Hes1 -knockout  
442 mice reveals plasticity of endodermal progenitors of the gut, bile duct, and pancreas. *J Clin*  
443 *Invest.* 2006;116:1484-1493.
- 444 6. Murtaugh LC, Stanger BZ, Kwan KM, et al. Notch signaling controls multiple steps of  
445 pancreatic differentiation. *Proc Natl Acad Sci U S A.* 2003;100:14920-14925.
- 446 7. Hidalgo-Sastre A, Brodylo RL, Lubeseder-Martellato C, et al. Hes1 controls exocrine cell  
447 plasticity and restricts development of pancreatic ductal adenocarcinoma in a mouse model.  
448 *Am J Pathol.* 2016;186:2934-2944.
- 449 8. Rovira M, Scott SG, Liss AS, et al. Isolation and characterization of centroacinar/terminal  
450 ductal progenitor cells in adult mouse pancreas. *Proc Natl Acad Sci U S A.* 2010;107:75-80.
- 451 9. Furuyama K, Kawaguchi Y, Akiyama H, et al. Continuous cell supply from a Sox9-expressing  
452 progenitor zone in adult liver, exocrine pancreas and intestine. *Nat Genet.* 2011;43:34-41.
- 453 10. Miyamoto Y, Maitra A, Ghosh B, et al. Notch mediates TGF alpha-induced changes in  
454 epithelial differentiation during pancreatic tumorigenesis. *Cancer Cell.* 2003;3:565-76.
- 455 11. Nakano Y, Negishi N, Gocho S, et al. Disappearance of centroacinar cells in the Notch ligand-

- 456 deficient pancreas. *Genes Cells*. 2015;20:500-511.
- 457 12. Gu G, Dubauskaite J, Melton DA. Direct evidence for the pancreatic lineage: NGN3+ cells  
458 are islet progenitors and are distinct from duct progenitors. *Development*. 2002;129:2447-  
459 2457.
- 460 13. Imayoshi I, Shimogori T, Ohtsuka T, et al. Hes genes and neurogenin regulate non-neural  
461 versus neural fate specification in the dorsal telencephalic midline. *Development*.  
462 2008;135:2531-2541.
- 463 14. Nishikawa Y, Kodama Y, Shiokawa M, et al. Hes1 plays an essential role in Kras-driven  
464 pancreatic tumorigenesis. *Oncogene*. 2019;38:4283-4296.
- 465 15. Gukovskaya AS, Gukovsky I. Autophagy and pancreatitis. *Am J Physiol Gastrointest Liver*  
466 *Physiol*. 2012;303:993-1003.
- 467 16. Arda HE, Benitez CM, Kim SK. Gene regulatory networks governing pancreas development.  
468 *Dev Cell*. 2013;25:5-13.
- 469 17. Mameishvili E, Serafimidis I, Iwaszkiewicz S, et al. Aldh1b1 expression defines progenitor  
470 cells in the adult pancreas and is required for Kras-induced pancreatic cancer. *Proc Natl Acad*  
471 *Sci U S A*. 2019;116:20679-20688.
- 472

473 **Figure Captions**

474

475 **Fig. 1**

476 ***Hes1* knockout in *Ptf1a*-positive progenitor cells does not affect fetal pancreatic development.**

477 Analysis at P0 in conditional *Hes1* knockout (*Hes1 cKO*) (*Ptf1a<sup>cre/+</sup>; Hes1<sup>fl/fl</sup>; Rosa26<sup>LacZ</sup>*) and  
478 control (Ctrl) (*Ptf1a<sup>+/+</sup>; Hes1<sup>fl/fl</sup>; Rosa26<sup>LacZ</sup>*, *Ptf1a<sup>cre/+</sup>; Hes1<sup>+/+</sup>; Rosa26<sup>LacZ</sup>* or *Ptf1a<sup>cre/+</sup>; Hes1<sup>fl/+</sup>;  
479 Rosa26<sup>LacZ</sup>*) mice. **a** Stereomicroscopic images, stereomicroscopic image of X-gal staining, and  
480 H&E staining of the pancreas. **b** Immunohistochemical staining for amylase, cytokeratin, insulin,  
481 and glucagon. There is no obvious difference between *Hes1 cKO* and control mice. Scale bars: 50  
482  $\mu\text{m}$ .

483

484 **Fig. 2**

485 **Transgenic *Notch1* expression in *Ptf1a*-positive progenitor cells does not affect fetal  
486 pancreatic development.**

487 Analysis of *Ptf1a<sup>cre/+</sup>; Rosa26<sup>NICD</sup>* and control mice (*Ptf1a<sup>+/+</sup>; Rosa26<sup>NICD</sup>*) at P0 (**a**) and P3 (**b** and  
488 **c**). Stereomicroscopic images, H&E staining, immunofluorescent staining for amylase, cytokeratin,  
489 insulin, and glucagon showed no obvious difference between *Ptf1a<sup>cre/+</sup>; Rosa26<sup>NICD</sup>* and control  
490 mice. Scale bars: 1000  $\mu\text{m}$  (**a**), 50  $\mu\text{m}$  (**a-c**).

491

492 **Fig. 3**

493 ***Hes1* knockout in *Ptf1a*-positive progenitor cells resulted in exocrine atrophy of the adult  
494 pancreatic tail.**

495 **a** Time-course analysis by X-gal staining in conditional *Hes1 cKO* (*Ptf1a<sup>cre/+</sup>; Hes1<sup>fl/fl</sup>; Rosa26<sup>LacZ</sup>*)  
496 and control (*Ptf1a<sup>cre/+</sup>; Hes1<sup>fl/+</sup>; Rosa26<sup>LacZ</sup>*) mice at indicated weeks of age. *Hes1 cKO* mice showed

497 atrophic changes in the pancreatic tail compared to control mice. **b** H&E staining and  
498 immunohistochemical staining for amylase, cytokeratin, insulin, and glucagon in *Hes1 cKO* mice  
499 and control mice at 4 weeks of age. Impaired development of exocrine cells and fat replacement  
500 was found in *Hes1 cKO* mice, whereas no change was observed in endocrine cells. Scale bars: 50  
501  $\mu\text{m}$  (**b**).

502

503 **Fig. 4**

504 ***Hes1* knockout in *Ptf1a*-positive progenitor cells induced more apoptotic cells in the**  
505 **pancreatic tail.**

506 **a** Immunohistochemical analysis of Ki67 and cleaved caspase3 in the pancreatic head and tail in  
507 *Hes1 cKO* (*Ptf1a<sup>cre/+</sup>;Hes1<sup>fl/fl</sup>*) and control (*Ptf1a<sup>cre/+</sup>;Hes1<sup>fl/+</sup>*) mice at age P0. Representative  
508 immunohistochemical images (**a**) and their graphic representation (**b**, **c**). Arrow heads show  
509 apoptotic cells in pancreas. Arrows show apoptotic cells in duodenum (positive control).  
510 Significantly more apoptotic cells were detected in the pancreatic tail in *Hes1 cKO* mice than in  
511 control mice (**a**, **c**), whereas there was no difference in the number of Ki67-positive cells (**a**, **b**).  
512 Scale bars: 50  $\mu\text{m}$  (**a**, Ki67 and Cleaved Caspase3 of pancreatic tail), 100  $\mu\text{m}$  (**a**, Cleaved Caspase3  
513 of pancreatic head). \*P < 0.05.

514

515 **Fig. 5**

516 ***Hes1* knockout in *Ptf1a*-positive progenitor cells induces reduction of centroacinar cells.**

517 **a** H&E staining and immunohistochemical images of *Hes1* and *ALDH1A1* in *Hes1 cKO*  
518 (*Ptf1a<sup>cre/+</sup>;Hes1<sup>fl/fl</sup>*) and control (Ctrl, *Ptf1a<sup>cre/+</sup>;Hes1<sup>fl/+</sup>*) mice at P0. Magnifications of the broken  
519 line are shown. Centroacinar cells expressed *Hes1* and *ALDH1A1* in control mice, whereas there  
520 was a vacant space in the center of acini of *Hes1 cKO* mice. **b**, **c** The ratio of acini without



521 centroacinar cells at P0 (b) and P3 (c) in the pancreatic head and tail of *Hes1 cKO* and control  
522 mice are shown. The ratio of acini without centroacinar cells was significantly higher in *Hes1 cKO*  
523 than in control mice at P0 (b). Centroacinar cell reduction was still observed in the pancreatic tail  
524 of *Hes1 cKO* mice at P3 (c). **d-f**: Microarray analysis of pancreatic head and tail tissue in *Hes1*  
525 *cKO* and control mice at P7. Expression of exocrine-related genes was reduced in the pancreatic  
526 tail of *Hes1 cKO* mice (d), whereas expression of endocrine-related genes was elevated (e)  
527 compared to in the control group or head of *Hes1 cKO* mice. Expression of *Aldh1*, a centroacinar  
528 cell marker, was lower in the pancreatic tail of *Hes1 cKO* mice (f). **g** Quantitative analysis of  
529 *Aldh1a1* mRNA expression in the pancreatic head and tail of *Hes1 cKO* and control mice. Scale  
530 bars: 50  $\mu\text{m}$  (a, H&E), 15  $\mu\text{m}$  (a, ALDH1A1). \*P < 0.05.

531

## 532 **Fig. 6**

533 **Transgenic *Notch1* expression compensates for the *Hes1* knockout phenotype in *Ptf1a*-**  
534 **positive progenitor cells.**

535 Analysis of *Ptf1a<sup>cre/+</sup>; Hes1<sup>ff</sup>; Rosa26<sup>NICD</sup>* mice and control (*Ptf1a<sup>+/+</sup>; Hes1<sup>ff</sup>; Rosa26<sup>NICD</sup>*) at P0  
536 (a) and at 16 weeks of age (b, c). **a** H&E staining showed almost normal pancreatic development  
537 in *Ptf1a<sup>cre/+</sup>; Hes1<sup>ff</sup>; Rosa26<sup>NICD</sup>* mice at P0, although some acini showed a vacant space in the  
538 center without centroacinar cells. **b, c** At 16 weeks, H&E staining, immunohistochemistry of  
539 amylase and cytokeratin, and immunofluorescent staining for insulin and glucagon showed normal  
540 pancreatic tissue development in *Ptf1a<sup>cre/+</sup>; Hes1<sup>ff</sup>; Rosa26<sup>NICD</sup>* mice compared to *Ptf1a<sup>+/+</sup>; Hes1<sup>ff</sup>;*  
541 *Rosa26<sup>NICD</sup>* mice. Scale bars: 50  $\mu\text{m}$  (a-c).

542

## 543 **Fig. 7**

544 ***Hes1* knockout in *Pdx1*-positive progenitor cells induces impaired exocrine development in**

545 **the pancreatic head and tail.**

546 **a** Analysis of *Pdx1-Cre;Hes1<sup>ff</sup>* mice and control (*Hes1<sup>ff</sup>*) mice at P0. Hematoxylin and eosin  
547 (H&E) staining showed normal exocrine/endocrine cells and some acini without centroacinar cells.

548 **b** The ratio of acini without centroacinar cells was higher in *Pdx1-Cre;Hes1<sup>ff</sup>* than control mice at  
549 P0. **c** Time-course analysis of *Pdx1-Cre;Hes1<sup>ff</sup>;Rosa26<sup>LacZ</sup>* and control (*Pdx1-*

550 *Cre;Hes1<sup>ff</sup>;Rosa26<sup>LacZ</sup>*) mice by X-gal staining at indicated weeks of age. Broken lines show the  
551 pancreas. X-gal staining showed gradual reduction of exocrine cells in *Pdx1-cre;Hes1<sup>ff</sup>;Rosa26<sup>LacZ</sup>*

552 mice. **d** Microscopic image of X-gal staining of pancreatic tissues in *Pdx1-Cre;Hes1<sup>ff</sup>;Rosa26<sup>LacZ</sup>*

553 and control (*Pdx1-Cre;Hes1<sup>ff</sup>;Rosa26<sup>LacZ</sup>*) mice at P0 and 8 weeks of age. Only endocrine cells

554 and a few exocrine cells were stained blue, and pancreatic tissue was replaced by non-stained

555 exocrine cells in both the pancreatic head and tail at 8 weeks of age. Scale bars: 50  $\mu\text{m}$  (**a, d**), 1000

556  $\mu\text{m}$  (**a**). An arrow head shows an islet (**d**).

557

558

## 559 **Supplementary Figure S1**

### 560 **Mouse strains**

561 **a** The protein-coding region of *Ptfla* was precisely replaced with that of *Cre*, encoding the

562 recombinase Cre. **b** *Hes1* is floxed by *loxP* and conditionally knocked out in the Cre recombinase

563 promoter site. **c** *Rosa-26*, *Lox-STOP-Lox*, and *LacZ* construct. LacZ expresses in the Cre

564 recombinase promoter site. **d** *Rosa-26*, *Lox-STOP-Lox*, and *NICD* construct. NICD expresses in

565 the Cre recombinase promoter site. **e** Cre recombinase is under the transcriptional control of the

566 mouse *Pdx1* promoter.

567

## 568 **Supplementary Figure S2**

569 **Hes1 immunohistochemistry**

570 Hes1 expression in pancreatic tissue was analyzed by immunohistochemistry in *Hes1 cKO*  
571 (*Ptf1a<sup>cre/+</sup>;Hes1<sup>ff</sup>;Rosa26<sup>LacZ</sup>*) and control (Ctrl, *Ptf1a<sup>+/+</sup>;Hes1<sup>ff</sup>;Rosa26<sup>LacZ</sup>*) mice at P0. Hes1  
572 expression was deleted in *Hes1 cKO* mice (**b**), while it was positive in the ducts and centroacinar  
573 cells of control mice (**a**).

574

575

576 **Supplementary Figure S3**

577 **Changes in body weight and blood glucose level**

578 Changes in body weight (**a**) and blood glucose level (**b**) after birth in *Hes1 cKO*  
579 (*Ptf1a<sup>cre/+</sup>;Hes1<sup>ff</sup>;Rosa26<sup>LacZ</sup>*) and control (Ctrl, *Ptf1a<sup>+/+</sup>;Hes1<sup>ff</sup>;Rosa26<sup>LacZ</sup>*) mice. The median  
580 and the standard error of mean are shown.

581

582 **Supplementary Figure S4**

583 ***Hes1* knockout in Ptf1a-positive progenitor cells.**

584 X-gal staining of *Hes1* conditional knockout mice (*Ptf1a<sup>cre/+</sup>;Hes1<sup>ff</sup>;Rosa26<sup>LacZ</sup>*) and control mice  
585 (*Ptf1a<sup>cre/+</sup>;Hes1<sup>ff/+</sup>;Rosa26<sup>LacZ</sup>*) at 4 weeks of age. **b** and **d** are a magnification of the broken line  
586 in **a** and **c**. Arrow head: islet, arrow: duct. Scale bars: 50  $\mu$ m (**b**, **d**).

587

588 **Supplementary Figure S5**

589 **a** Western blot analysis for LC3-I and its lipidated form LC3-II. We found expression of LC3-I  
590 but not its lipidated form LC3-II in both pancreatic head and tail of *Hes1 cKO* mice and control  
591 mice at P4.

592

593 **Supplementary Figure S6**

594 **a** Immunofluorescence images of Hes1 and Aldh1a1 in *Hes1 cKO* (*Ptfla<sup>cre/+</sup>;Hes1<sup>fl/fl</sup>*) and control  
595 (Ctrl, *Ptfla<sup>+/+</sup>;Hes1<sup>fl/fl</sup>*) mice at P3. Scale bars: 50  $\mu$ m. **b** Microarray analysis of pancreatic head and  
596 tail tissues of *Hes1 cKO* and control mice at P7. A heatmap of genes related to pancreatic  
597 development is shown.

598

599 **Supplementary Figure S7**

600 **a** FACS isolation of Aldh-positive cells with Aldefluor reagent. FACS gating was established by  
601 negative control. The number of Aldh-positive cells were decreased in *Hes1 cKO*  
602 (*Ptfla<sup>cre/+</sup>;Hes1<sup>fl/fl</sup>*) mice compared with that in control mice at P7 (**b**). The number of organoid  
603 formation from pancreatic cells (**c, d**). \*P < 0.05.

604

605 **Supplementary Figure S8**

606 **a** H&E staining and immunohistochemical staining for Hes5 and Hey1 of control mice,  
607 *Ptfla<sup>cre/+</sup>;Hes1<sup>fl/fl</sup>* mice (*cKO*), *Ptfla<sup>cre/+</sup>;Rosa26<sup>NICD</sup>* mice, and *Ptfla<sup>cre/+</sup>;Hes1<sup>fl/fl</sup>;Rosa26<sup>NICD</sup>* mice  
608 at P0. Marked increase of Hes5 expression was observed in *Ptfla<sup>cre/+</sup>;Hes1<sup>fl/fl</sup>;Rosa26<sup>NICD</sup>* mice.  
609 Scale bars: 50  $\mu$ m.

610

611 **Supplementary Table 1.**

612 Primary antibodies used in this study.

613

614

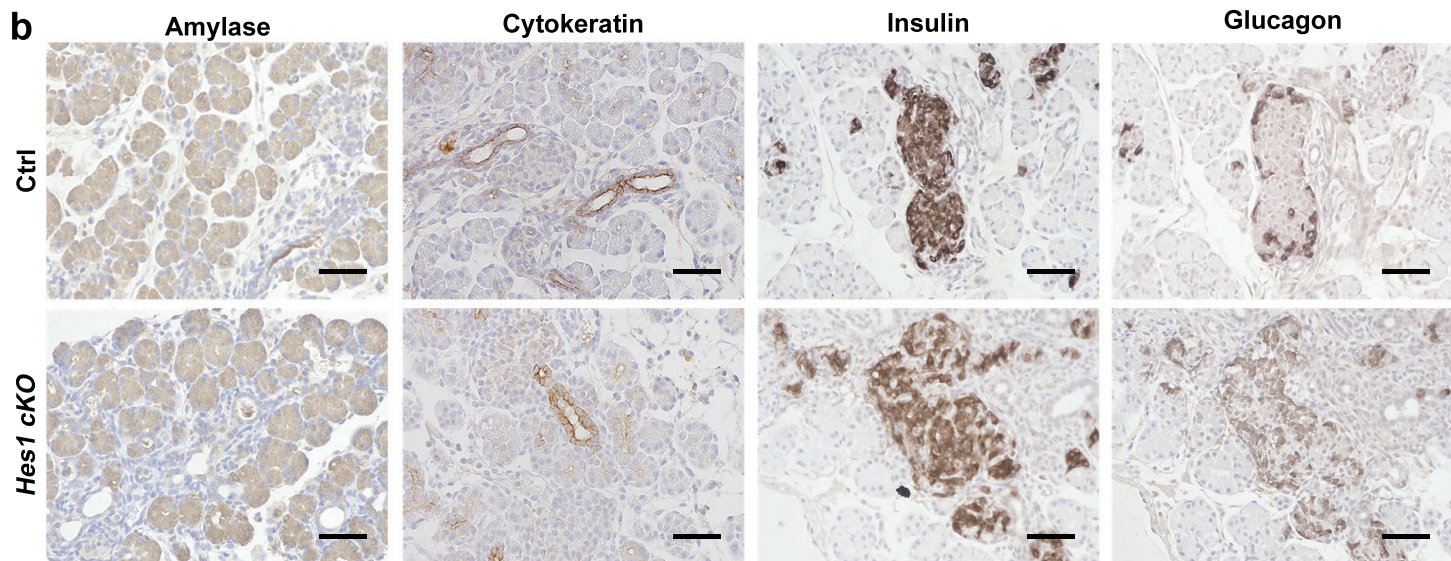
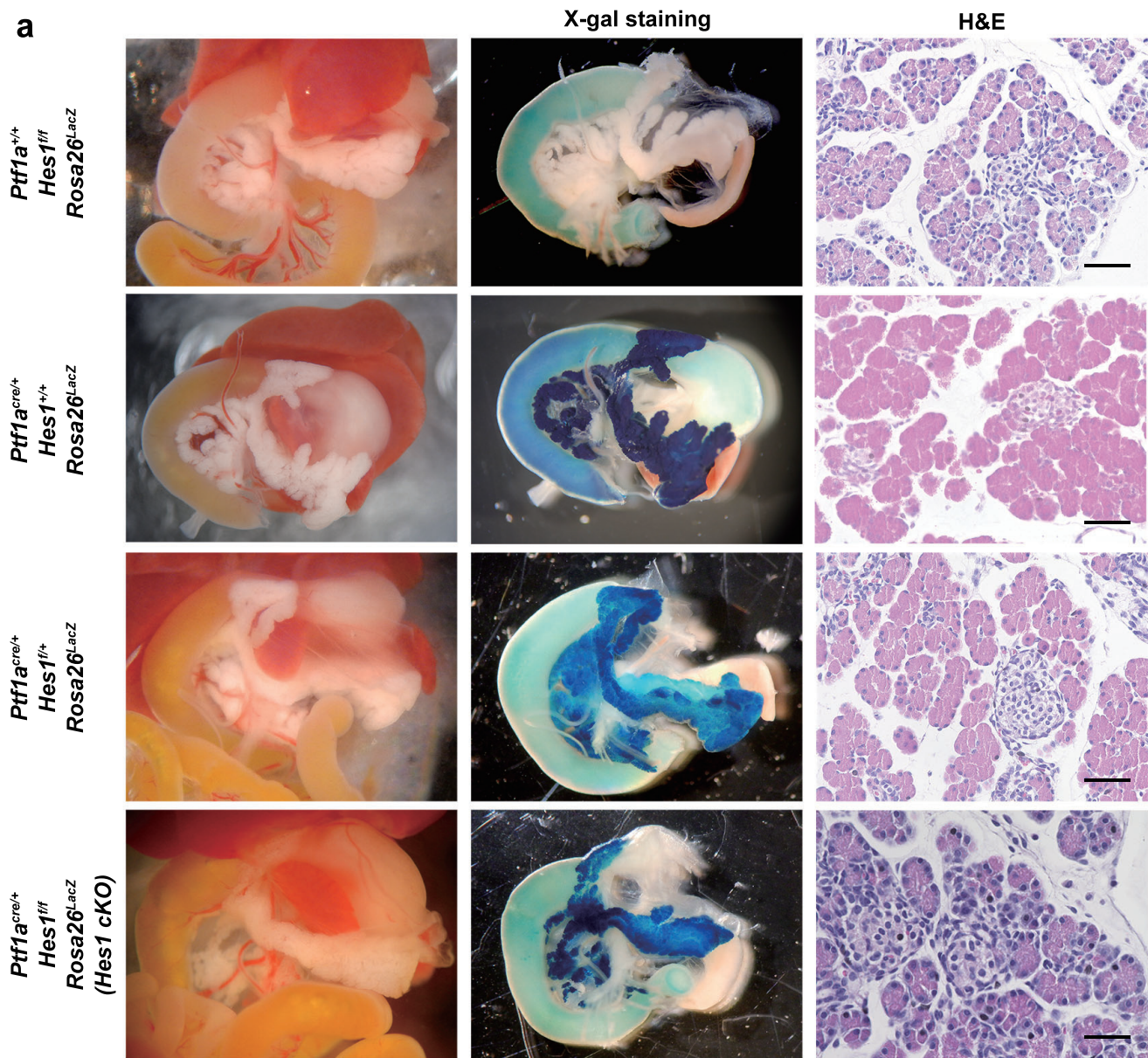


**Fig. 1**

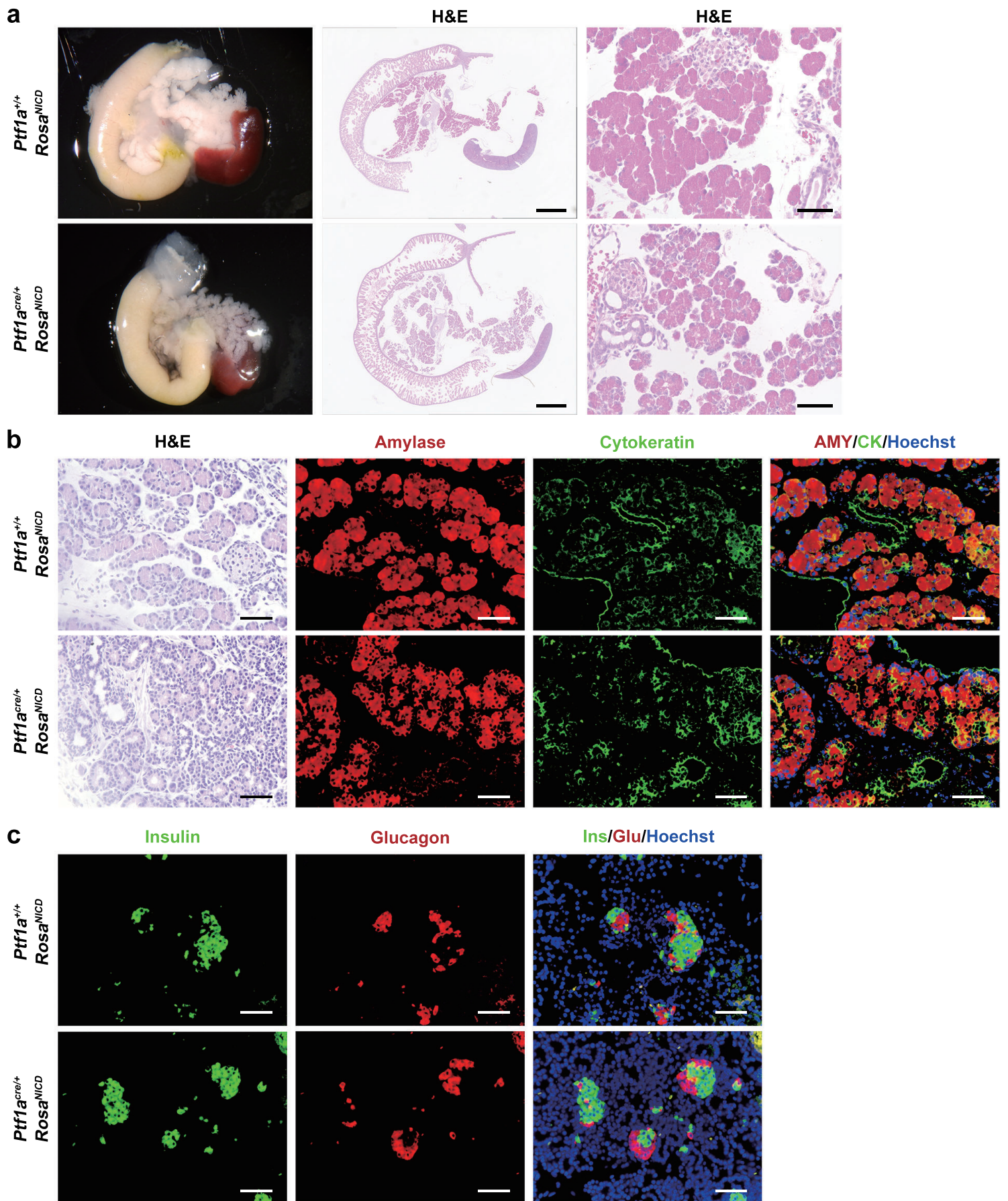


**Fig. 2**

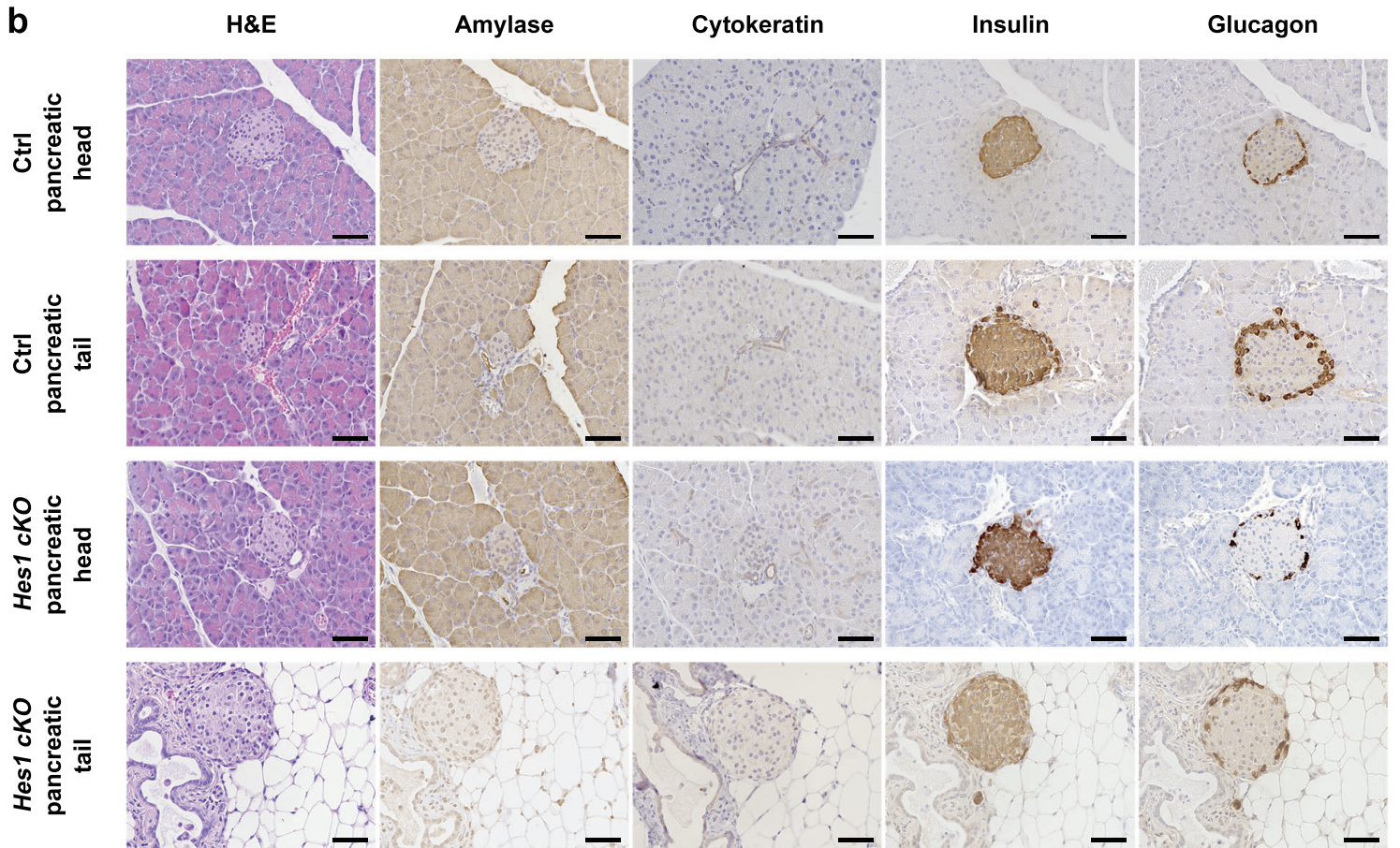
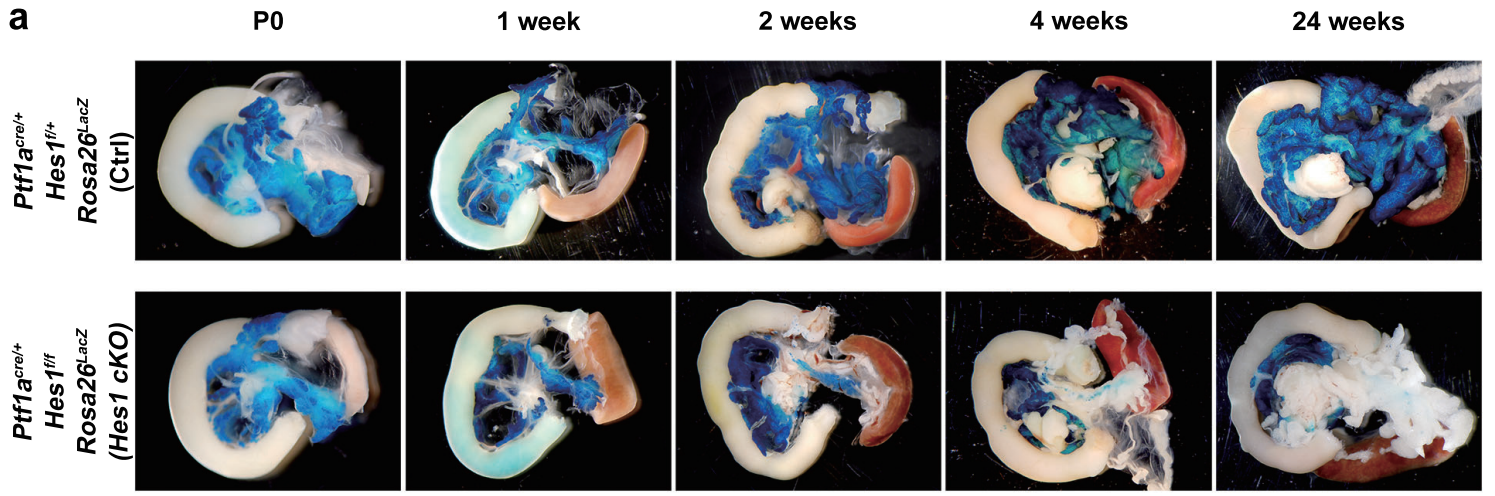


**Fig. 3**

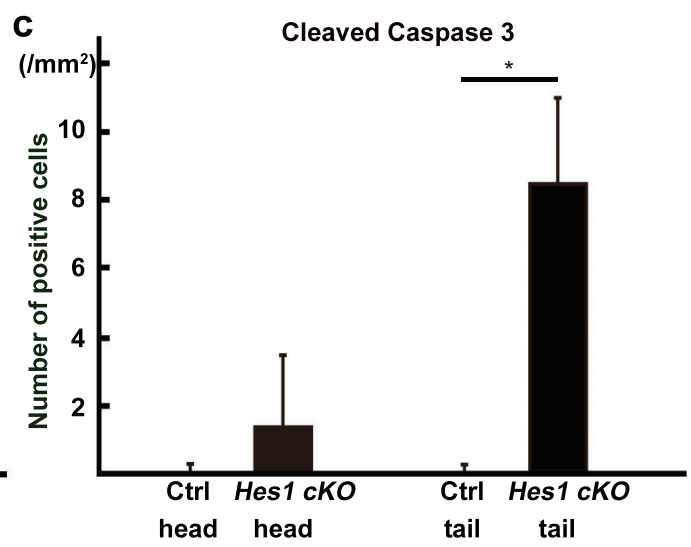
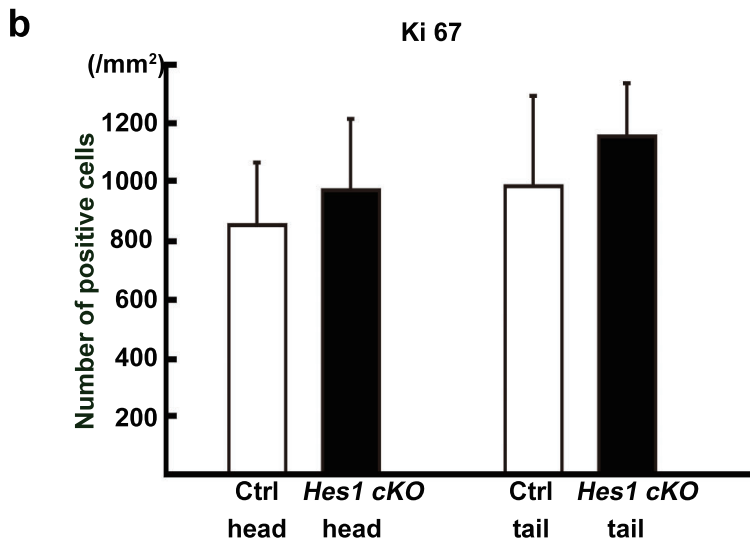
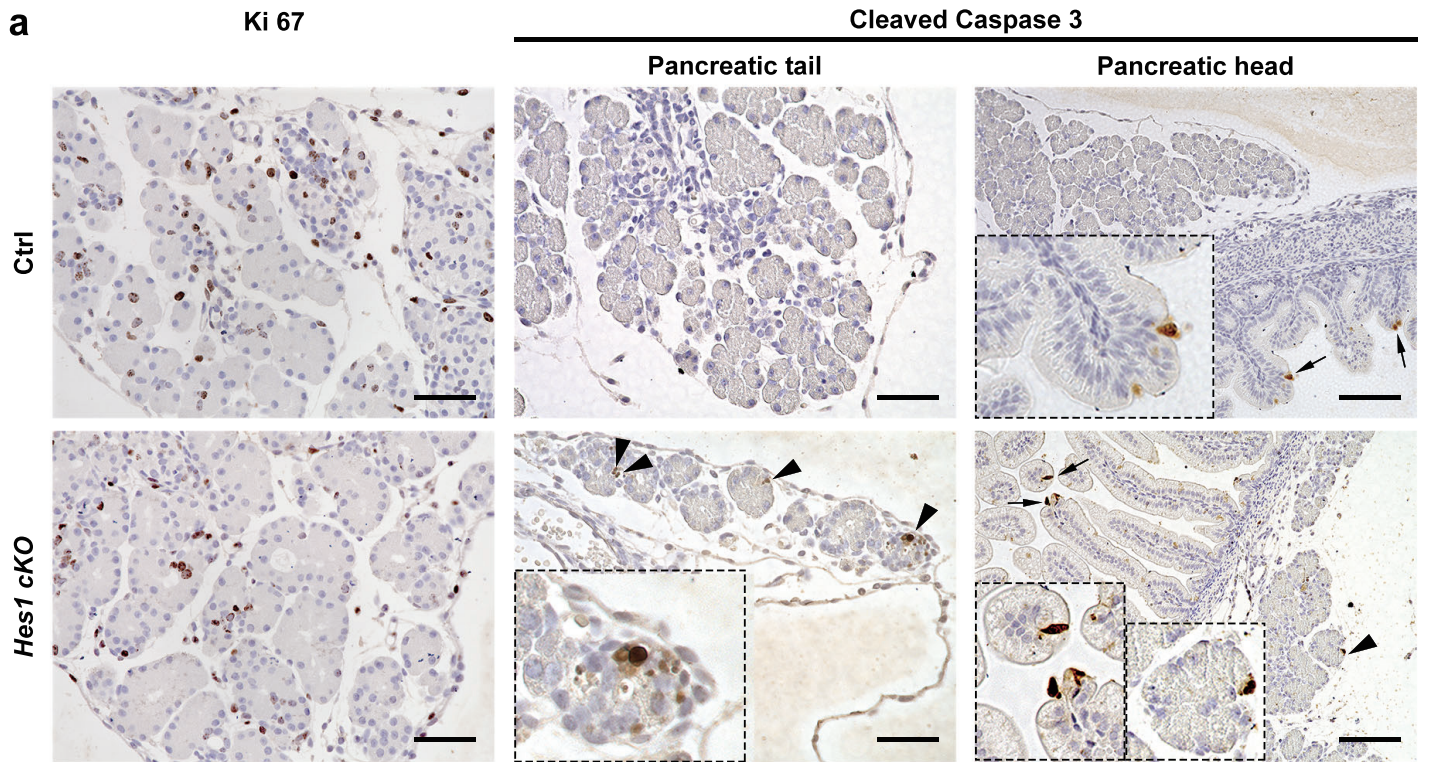


**Fig. 4**



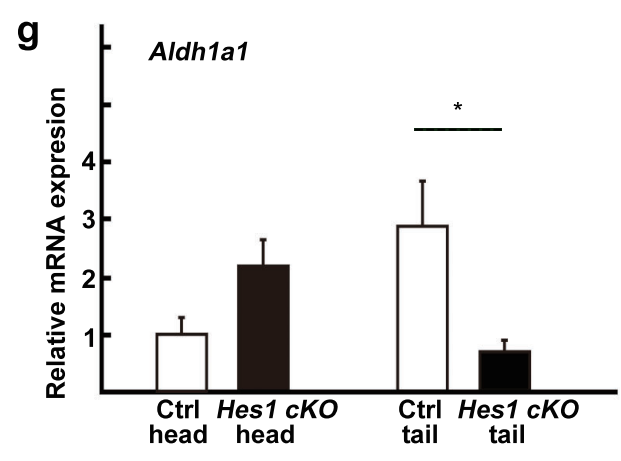
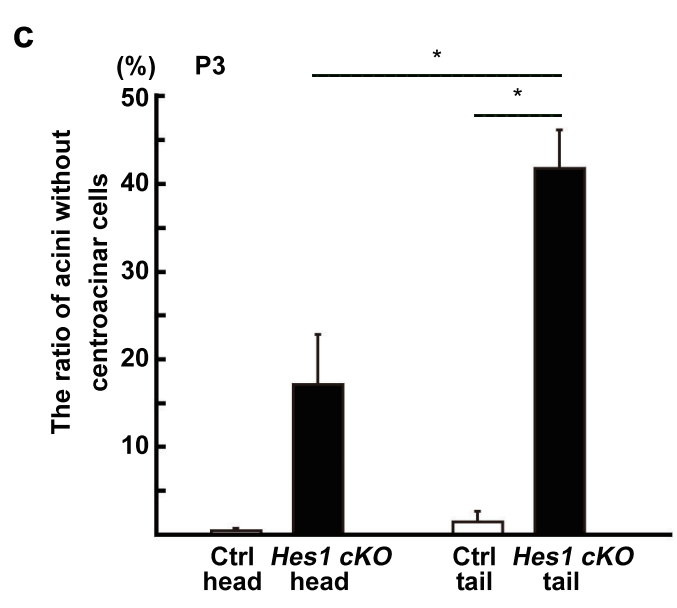
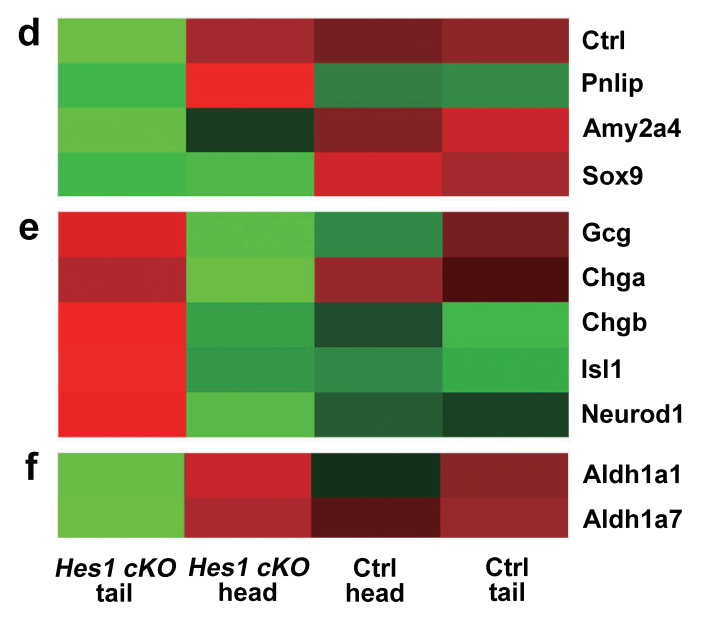
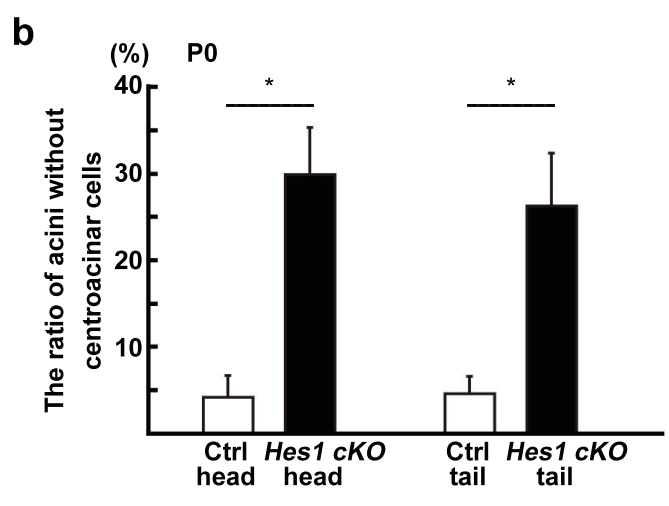
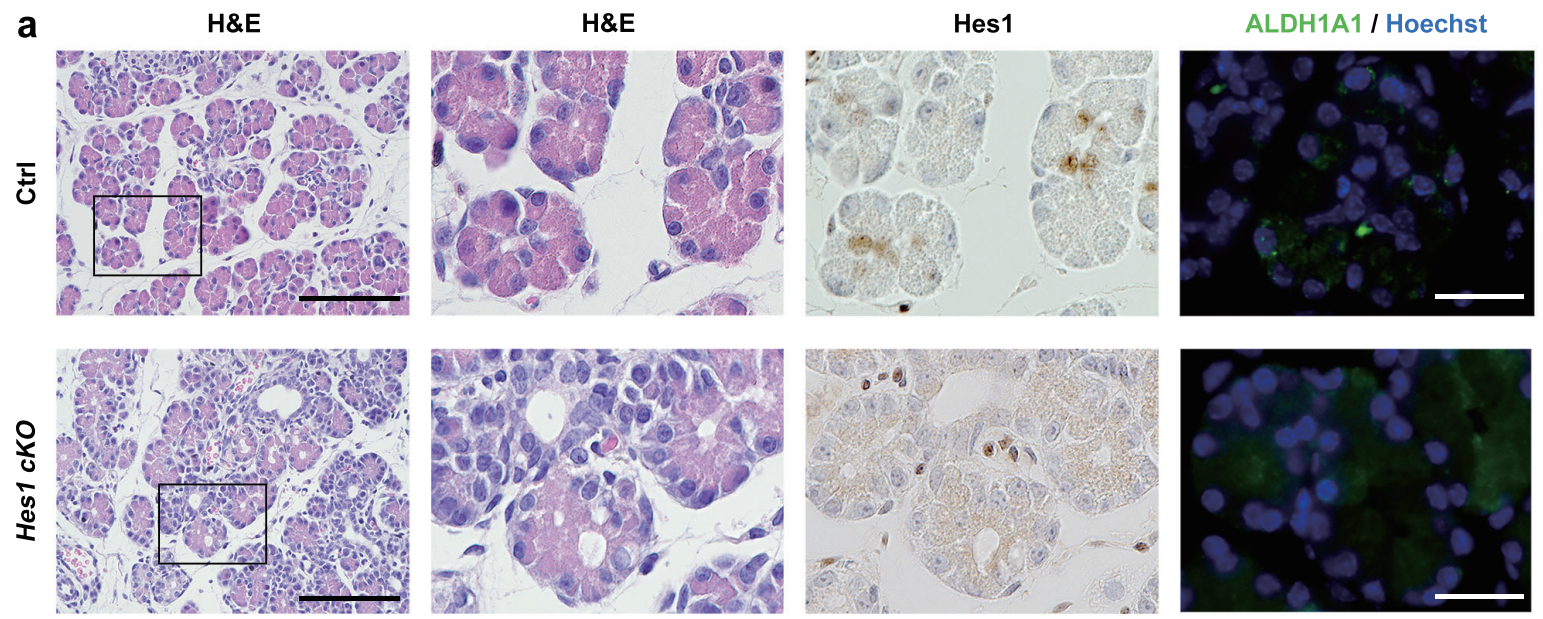


**Fig. 5**

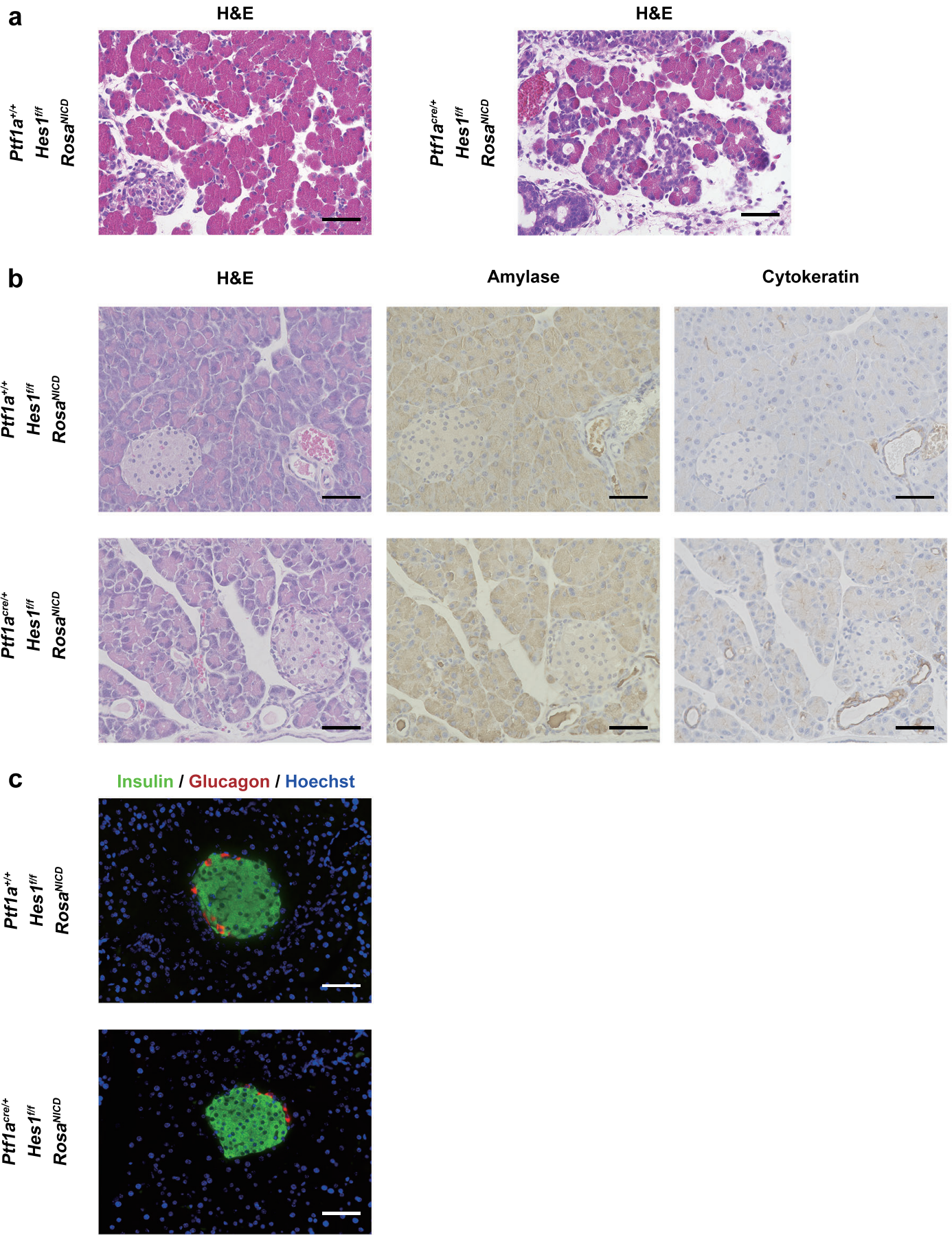


**Fig. 6**

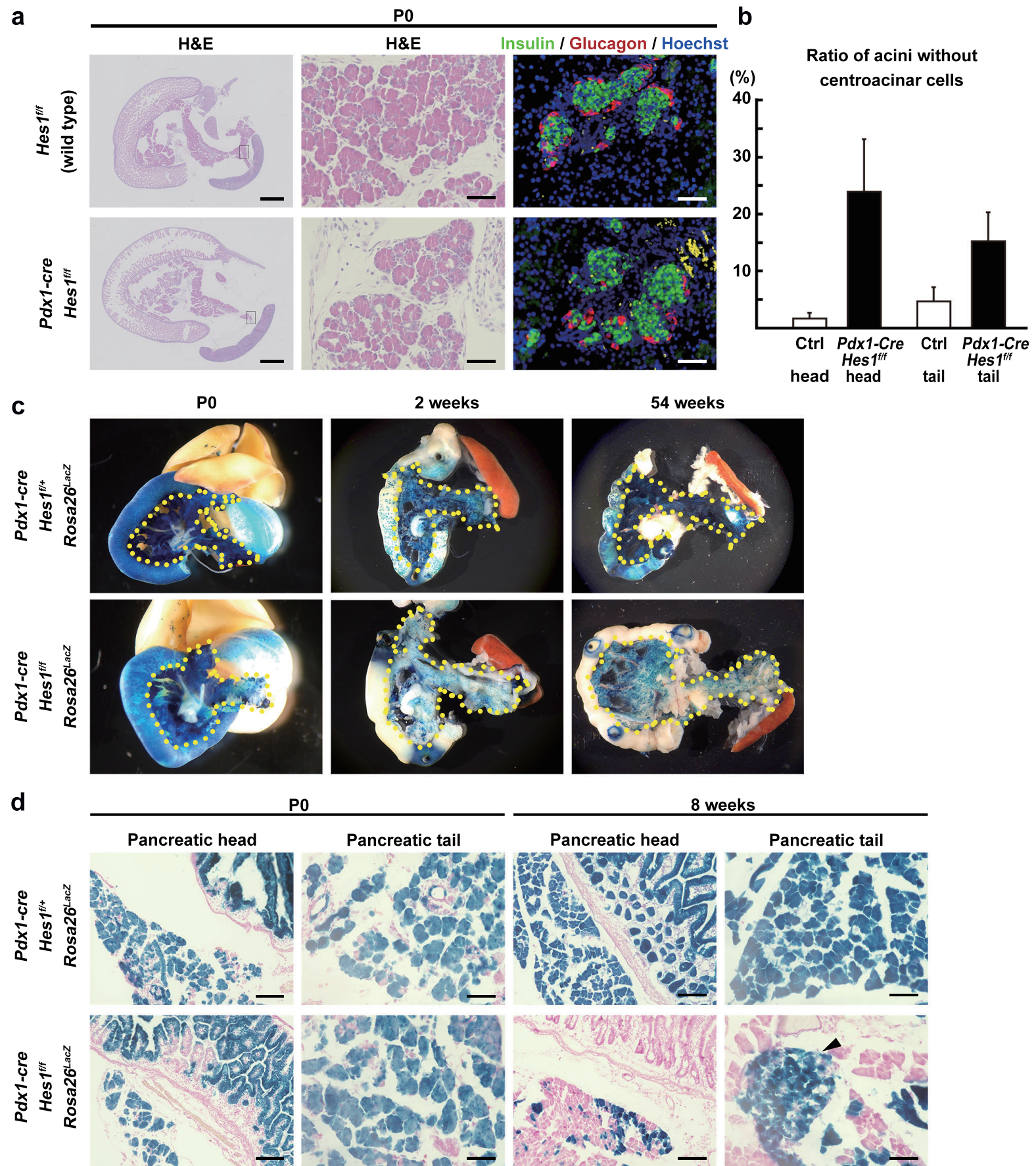
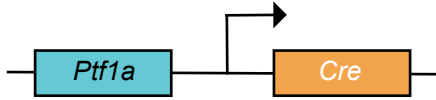
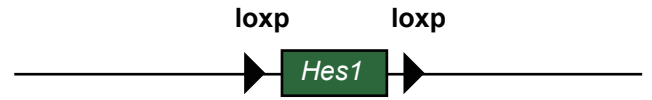


Fig. 7

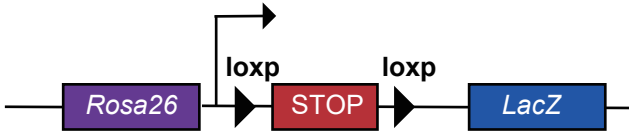
**a** *Ptf1a*<sup>cre/+</sup>



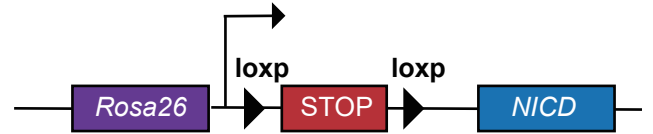
**b** *Hes1*<sup>fl/fl</sup>



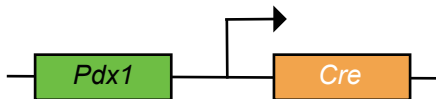
**c** *Rosa26*<sup>LacZ</sup>



**d** *Rosa26*<sup>NICD</sup>



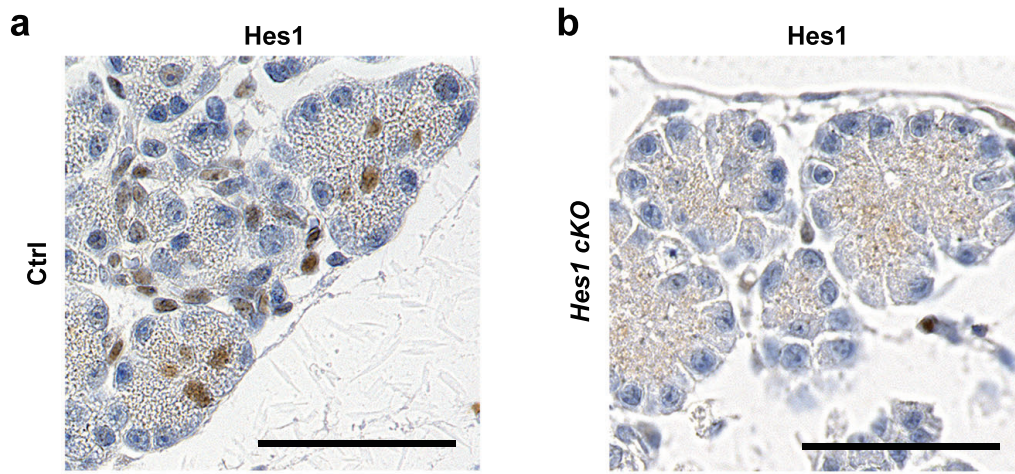
**e** *Pdx1*-Cre



## Supplementary Figure S1

### Mouse strains

**a** The protein-coding region of *Ptf1a* was precisely replaced with that of *Cre*, encoding the recombinase Cre. **b** *Hes1* is floxed by *loxP* and conditionally knocked out in the Cre recombinase promoter site. **c** *Rosa-26*, *Lox-STOP-Lox*, and *LacZ* construct. *LacZ* expresses in the Cre recombinase promoter site. **d** *Rosa-26*, *Lox-STOP-Lox*, and *NICD* construct. *NICD* expresses in the Cre recombinase promoter site. **e** Cre recombinase is under the transcriptional control of the mouse *Pdx1* promoter.

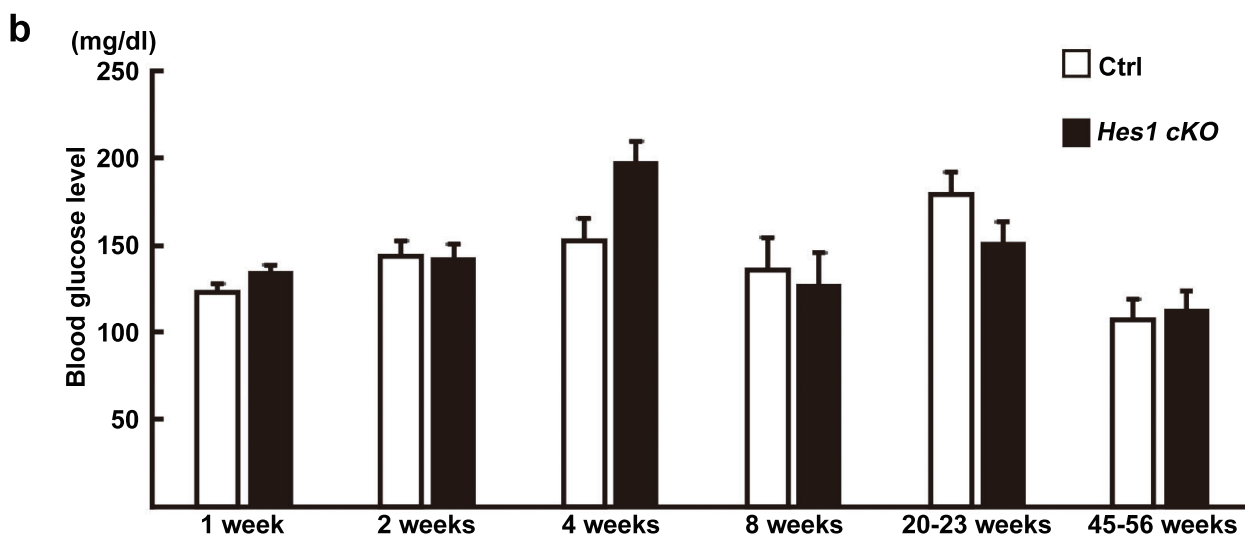
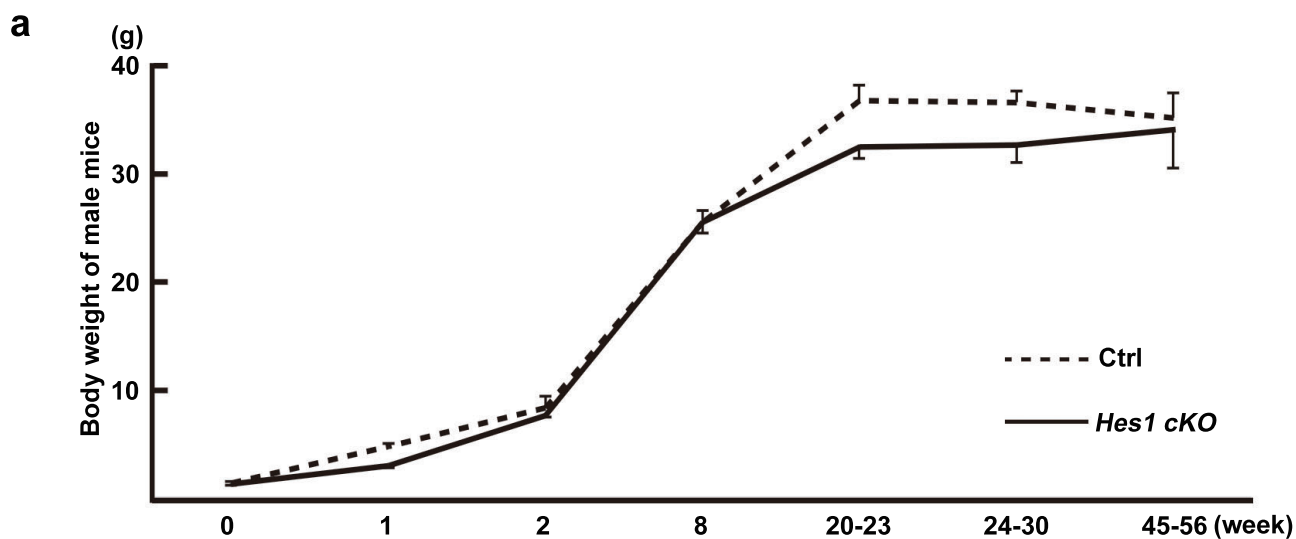


## Supplementary Figure S2

### Hes1 immunohistochemistry

Hes1 expression in pancreatic tissue was analyzed by immunohistochemistry in *Hes1 cKO* (*Ptfla<sup>cre/+</sup>;Hes1<sup>fl/fl</sup>;Rosa26<sup>LacZ</sup>*) and control (Ctrl, *Ptfla<sup>+/+</sup>;Hes1<sup>fl/fl</sup>;Rosa26<sup>LacZ</sup>*) mice at P0.

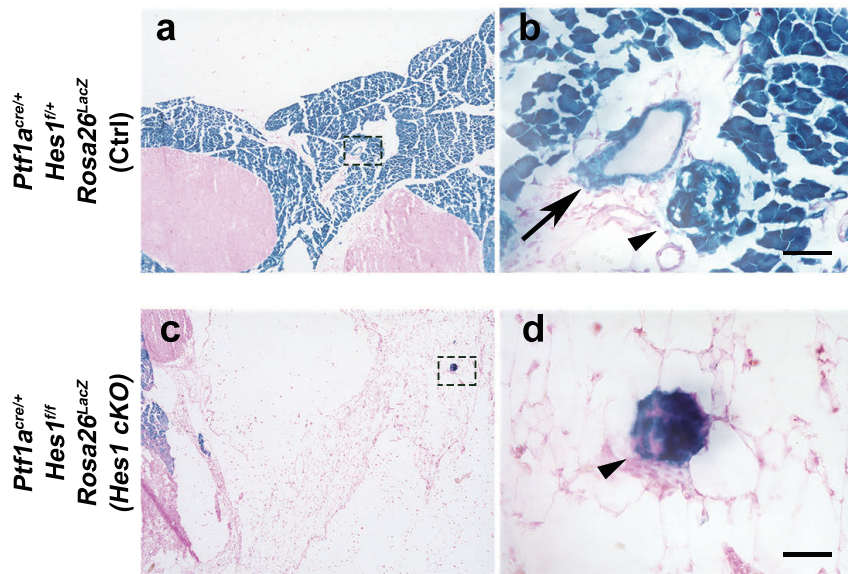
Hes1 expression was deleted in *Hes1 cKO* mice (b), while it was positive in the ducts and centroacinar cells of control mice (a).



### Supplementary Figure S3

#### Changes in body weight and blood glucose level

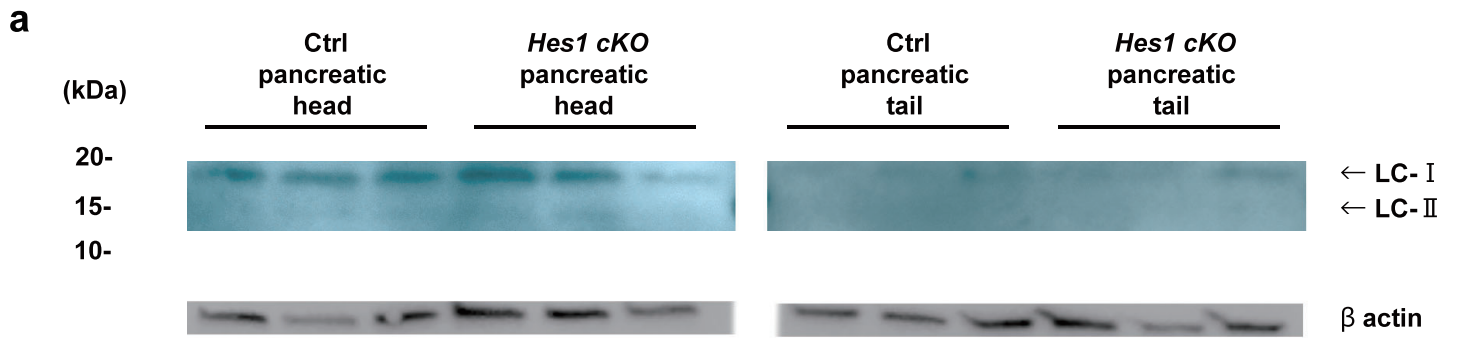
Changes in body weight (**a**) and blood glucose level (**b**) after birth in *Hes1 cKO* (*Ptfl1<sup>cre/+</sup>;Hes1<sup>fl/fl</sup>;Rosa26<sup>LacZ</sup>*) and control (Ctrl, *Ptfl1<sup>+/+</sup>;Hes1<sup>fl/fl</sup>;Rosa26<sup>LacZ</sup>*) mice. The median and the standard error of mean are shown.



#### Supplementary Figure S4

##### ***Hes1* knockout in *Ptf1a*-positive progenitor cells.**

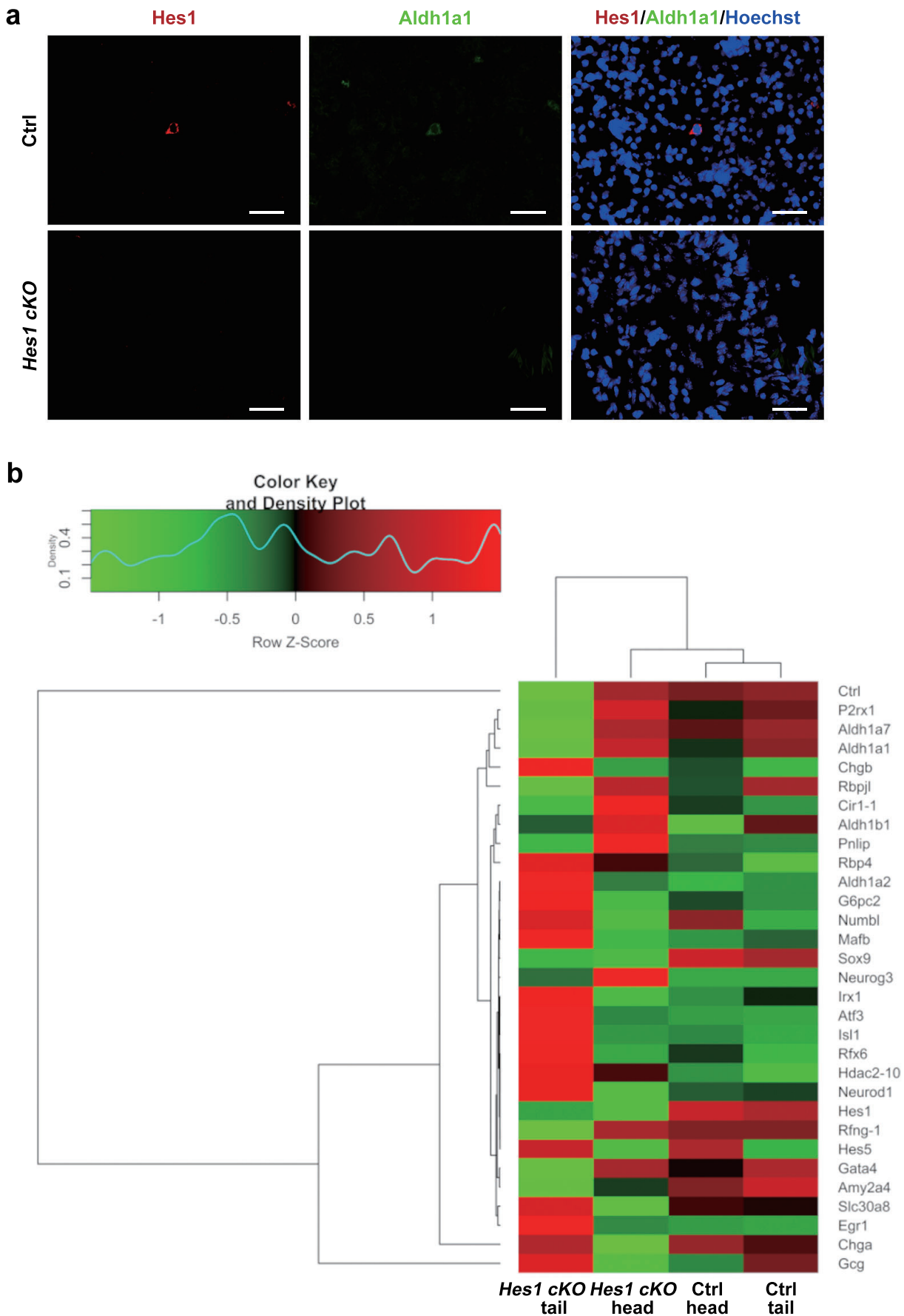
X-gal staining of *Hes1* conditional knockout mice ( $Ptf1a^{cre/+}; Hes1^{fl/fl}; Rosa26^{LacZ}$ ) and control mice ( $Ptf1a^{cre/+}; Hes1^{fl/+}; Rosa26^{LacZ}$ ) at 4 weeks of age. **b** and **d** are a magnification of the broken line in **a** and **c**. Arrow head: islet, arrow: duct. Scale bars: 50  $\mu$ m (**b**, **d**).



**Supplementary Figure S5**

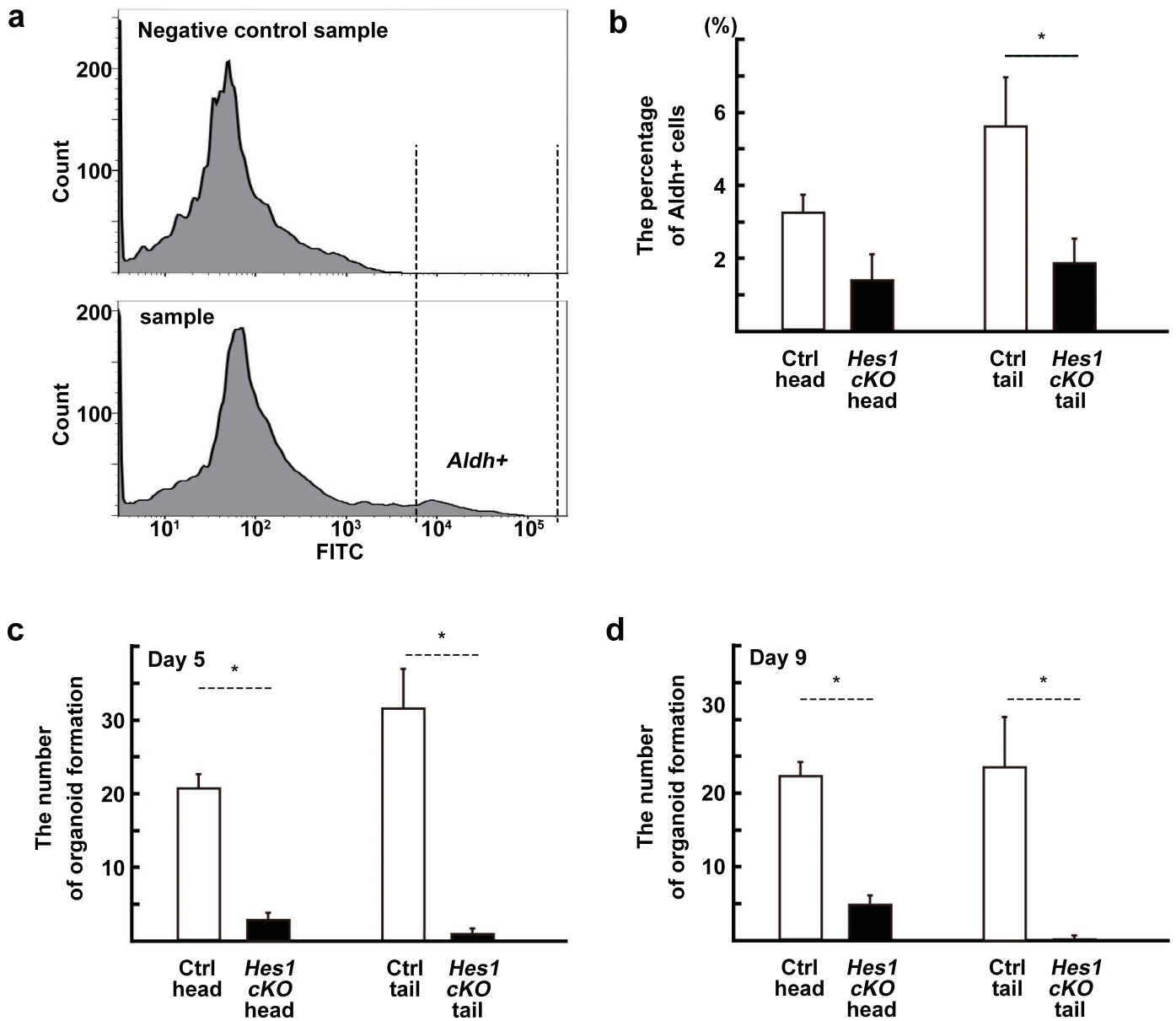
**a** Western blot analysis for LC3-I and its lipidated form LC3-II. We found expression of LC3-I but not its lipidated form LC3-II in both pancreatic head and tail of *Hes1 cKO* mice and control mice at P4.





### Supplementary Figure S6

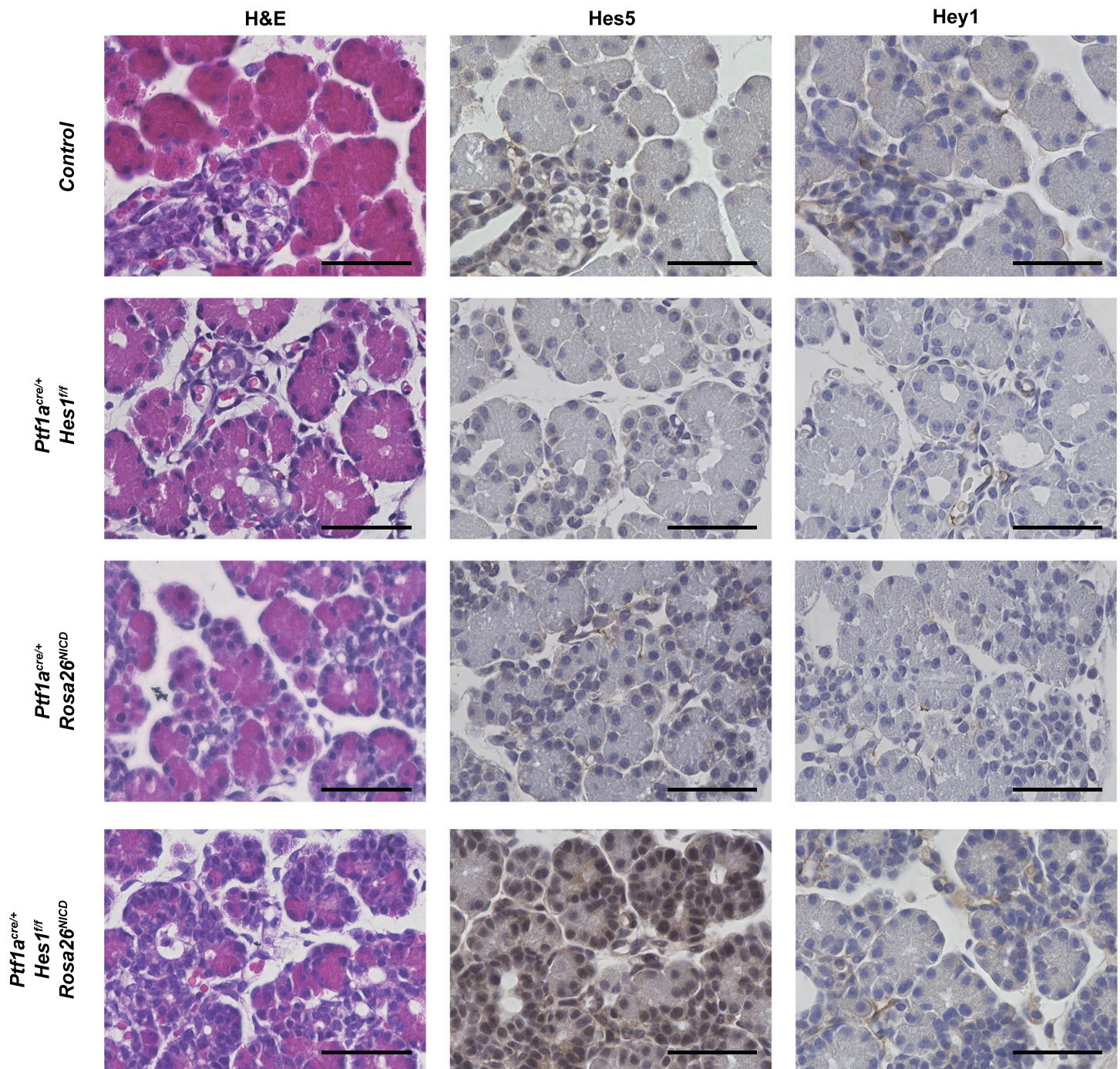
**a** Immunofluorescence images of Hes1 and Aldh1a1 in *Hes1 cKO* (*Ptfl1a<sup>cre/+</sup>;Hes1<sup>fl/fl</sup>*) and control (Ctrl, *Ptfl1a<sup>+/+</sup>;Hes1<sup>fl/fl</sup>*) mice at P3. Scale bars: 50  $\mu$ m. **b** Microarray analysis of pancreatic head and tail tissues of *Hes1 cKO* and control mice at P7. A heatmap of genes related to pancreatic development is shown.



### Supplementary Figure S7

a FACS isolation of *Aldh*-positive cells with Aldefluor reagent. FACS gating was established by negative control. The number of *Aldh*-positive cells were decreased in *Hes1* cKO (*Ptf1a<sup>cre/+</sup>; Hes1<sup>fl/fl</sup>*) mice compared with that in control mice at P7 (b). The number of organoid formation from pancreatic cells (c, d). \*P < 0.05.

a



### Supplementary Figure S8

a H&E staining and immunohistochemical staining for Hes5 and Hey1 of control mice, *Ptf1a*<sup>cre/+</sup>;*Hes1*<sup>ff</sup> mice (*cKO*), *Ptf1a*<sup>cre/+</sup>;*Rosa26*<sup>NICD</sup> mice, and *Ptf1a*<sup>cre/+</sup>;*Hes1*<sup>ff</sup>;*Rosa26*<sup>NICD</sup> mice at P0. Marked increase of Hes5 expression was observed in *Ptf1a*<sup>cre/+</sup>;*Hes1*<sup>ff</sup>;*Rosa26*<sup>NICD</sup> mice. Scale bars: 50  $\mu$ m.

Antigen	Species	Source	Catalog number	Dilution	Antigen retrieval
ALDH1A1	Rabbit	Abcam	ab52492	1:100	autoclave with ph6.0 citrate buffer
Amylase	Rabbit	Abcam	ab21156	1:300	microwave with ph6.0 citrate buffer
Cleaved caspase-3	Rabbit	Cell signaling	9664S	1:400	microwave with ph6.0 citrate buffer
Cytokeratin	Mouse	Dako	M3515	1:100	microwave with ph6.0 citrate buffer
Glucagon	Rabbit	Dako	A0565	1:300	none
Hes1	Rabbit	Gifted from Mr. Sudo (Toray, Japan)		1:5000	autoclave with ph6.0 citrate buffer
Hes1	Rabbit	Santa Cruz	SC-25392	1:400	autoclave with ph6.0 citrate buffer
Hes5	Rabbit	Abcam	ab194111	1:500	microwave with ph9.0 Tris / EDTA buffer
Heyl	Rabbit	Abcam	ab22614	1:200	microwave with ph9.0 Tris / EDTA buffer
Insulin	Guinea pig	Dako	A0564	1:400	none
Ki-67	Rabbit	Dako	M7249	1:400	microwave with ph6.0 citrate buffer

**Supplementary Table 1.**  
Primary antibodies used in this study.